

# Study of Static Wormhole Solutions in $F(T, T_G)$ Gravity

M. Sharif <sup>\*</sup> and Kanwal Nazir <sup>† ‡</sup>

Department of Mathematics, University of the Punjab,  
Quaid-e-Azam Campus, Lahore-54590, Pakistan.

## Abstract

In this paper, we investigate static spherically symmetric wormhole solutions in the background of  $F(T, T_G)$  gravity ( $T$  is the torsion scalar and  $T_G$  represents teleparallel equivalent of the Gauss-Bonnet term). We study the wormhole solutions by assuming four different matter contents, a specific redshift function and a particular  $F(T, T_G)$  model. The behavior of null/weak energy conditions for these fluids is analyzed graphically. It turns out that wormhole solutions can be obtained in the absence of exotic matter for some particular regions of spacetime. We also explore stability of wormhole solutions through equilibrium condition. It is concluded that there exist physically acceptable wormhole solutions for anisotropic, isotropic and traceless fluids.

**Keywords:** Wormhole solutions;  $F(T, T_G)$  gravity.

**PACS:** 04.50.Kd; 95.35.+d;

## 1 Introduction

The current accelerated expanding behavior of the universe is confirmed through several cosmological observations. The rapid rate of expansion indi-

---

<sup>\*</sup>msharif.math@pu.edu.pk

<sup>†</sup>awankanwal@yahoo.com

<sup>‡</sup>On leave from Department of Mathematics, Lahore College for Women University, Lahore-54000, Pakistan.

cates the presence of an anonymous force other than dark matter and baryonic matter in the universe. This mysterious force is labeled as dark energy (DE) which is equally scattered in the universe with negative pressure. Its mysterious nature can be explained through two renowned proposals. The first modifies the matter part while the second establishes the gravitational modification of the Einstein-Hilbert action leading to modified theories such as Gauss-Bonnet (GB) theory [1],  $f(R)$  theory ( $R$  represents the Ricci scalar) [2],  $F(T)$  theory [3],  $f(R, \mathcal{T})$  theory ( $\mathcal{T}$  defines trace of the energy-momentum tensor) [4] etc. Recently, another modification is introduced by incorporating  $T$  and  $T_{\mathcal{G}}$  known as  $F(T, T_{\mathcal{G}})$  gravity.

The  $F(T, T_{\mathcal{G}})$  theory is an extension of  $F(T)$  theory which is obtained by inserting the higher-order torsion invariants in the action. This is a torsion based modification with no curvature formulation. The motivation behind this extension is that in curvature based theory such as  $f(R)$  theory, higher-order curvature corrections like GB term  $\mathcal{G}$  and function  $f(\mathcal{G})$  are introduced in the action. On the same pattern, one can construct torsion based theory by involving higher-order torsion corrections terms in the action. A lot of work has been done to study different cosmological features using this theory [5]-[7]. The study of different matter contents is of great interest in modified theories. These matter distributions are helpful in explaining the matter contents of the astronomical objects like wormholes.

A wormhole is known as a hypothetical path like a tunnel or bridge that provides a connection between two different regions of the universe apart from one another. The existence of a realistic wormhole which satisfies the energy conditions has always been a challenging issue. Dynamical wormhole solutions [8], traversable wormholes [9], brane wormholes [10], generalized Chaplygin gas [11] etc are used to minimize the violation of energy conditions especially null energy condition (NEC). Rahaman et al. [12] studied wormhole solutions by considering noncommutative geometry and noticed the presence of asymptotically flat solutions for four dimensions. Abreu and Sasaki [13] explored the effects of energy conditions through noncommutative wormhole in the absence of exotic matter.

A comprehensive study of wormhole solutions has been done in modified theories. Lobo and Oliveira [14] studied wormhole solutions with different fluids in  $f(R)$  theory and explored energy conditions. Böhmer et al. [15] considered a particular model to derive traversable wormhole solutions in  $F(T)$  gravity and found that there exists a physically acceptable wormhole. Sharif and Rani [16] assumed a particular shape function as well as  $F(T)$  model with

noncommutative geometry and found that energy conditions violate due to the presence of effective energy-momentum tensor but noncommutative geometry does not play any role in this violation. We discussed wormhole solutions with noncommutative geometry in  $F(T, T_G)$  gravity and concluded that effective energy-momentum tensor is responsible for the violation of energy conditions [17].

Sharif and Rani [18] explored dynamical wormhole solutions in the same gravity using anisotropic matter distribution. Sharif and Zahra [19] discussed some specific solutions in  $f(R)$  gravity with isotropic, anisotropic and barotropic fluids and found that physically acceptable wormholes exist only for barotropic fluid in some particular regions. Sharif and Ikram [20] explored energy conditions for static wormhole solutions with same fluids in  $F(\mathcal{G})$  gravity. Zubair et al. [21] assumed the same fluids in  $F(R, \mathcal{T})$  gravity and found that realistic and stable wormhole solutions exist only for anisotropic case.

In this paper, we study static wormhole solutions in  $F(T, T_G)$  gravity with four matter contents. The paper is arranged as follows. In section **2**, we provide necessary formalism of wormhole geometry as well as energy conditions in this theory. Section **3** explores the structure and existence of the wormhole through shape function, NEC and weak energy condition (WEC) for four types of fluids and a specific  $F(T, T_G)$  model. In section **4**, we analyze stability of the wormhole solutions through equilibrium condition. Finally, we conclude our results.

## 2 Formalism of $F(T, T_G)$ Theory

In this section, we formulate the field equations in the framework of  $F(T, T_G)$  gravity and provide an overview of the energy conditions as well as wormhole geometry.

### 2.1 $F(T, T_G)$ Gravity

The tetrad field  $e_a(x^\mu)$  has a fundamental role in  $F(T)$  as well as  $F(T, T_G)$  gravity. Trivial tetrad is the simplest one expressed as  $e_a = \partial_\mu \delta^\mu_a$  and  $e^b = \partial^\mu \delta_\mu^b$ , where  $\delta^\mu_a$  is the Kronecker delta. These are not commonly used because they provide zero torsion. The non-trivial tetrad have different behavior, so they are more supportive in describing teleparallel theory. These tetrad can

be represented as

$$h_a = \partial_\mu h_a^\mu, \quad h^b = dx^\mu h_\mu^b,$$

satisfying

$$h^a_\mu h_b^\mu = \delta_b^a, \quad h^a_\mu h_a^\nu = \delta_\mu^\nu.$$

The metric tensor can also be expressed in the product of tetrad fields as

$$g_{\mu\nu} = \eta_{ab} h_\mu^a h_\nu^b,$$

where  $\eta_{ab} = \text{diag}(1, -1, -1, -1)$  is the Minkowski metric. The coordinates on manifold are represented by Greek indices  $(\mu, \nu, \dots)$  while coordinates on tangent space are characterized by Latin indices  $(a, b, \dots)$ .

The Weitzenböck connection  $\omega^a_b(x^\mu)$  that describes parallel transportation, has the following form

$$\omega_{ab}^c = h^c_\mu h^{\mu}_{a,b}.$$

The structure coefficients  $\mathcal{C}_{ab}^c$  are defined as

$$[h_a, h_b] = h_c \mathcal{C}_{ab}^c,$$

where

$$\mathcal{C}_{ab}^c = h^\nu_b h^\mu_a (h^c_{\mu,\nu} - h^c_{\nu,\mu}).$$

Similarly, we can express the torsion as well as curvature tensors as

$$\begin{aligned} T_{bc}^a &= -\omega_{bc}^a + \omega_{cb}^a - \mathcal{C}_{bc}^a, \\ R_{bcd}^a &= -\omega_{bc}^e \omega_{ed}^a + \omega_{bd,c}^a + \omega_{bd}^e \omega_{ec}^a - \mathcal{C}_{cd}^e \omega_{be}^a - \omega_{bc,d}^a. \end{aligned}$$

The contorsion tensor is defined by

$$\mathcal{K}_{abc} = \frac{1}{2}(-T_{bca} - T_{abc} + T_{cab}) = -\mathcal{K}_{bac}.$$

Finally, the torsion scalars  $T$  and  $T_{\mathcal{G}}$  take the form

$$\begin{aligned} T &= \frac{1}{4} T^{abc} T_{abc} - T_{ab}{}^a T^c{}_c + \frac{1}{2} T^{abc} T_{cba}, \\ T_{\mathcal{G}} &= (2\mathcal{K}^{a3}{}_{eb} \mathcal{K}^{a_1 a_2}{}_a \mathcal{K}^{ea_4}{}_f \mathcal{K}^f{}_{cd} + \mathcal{K}^{a_2}{}_b \mathcal{K}^{a_1}{}_{ea} \mathcal{K}^{a_3}{}_{fc} \mathcal{K}^{fa_4}{}_d + 2\mathcal{K}^{a_3}{}_{eb} \\ &\times \mathcal{K}^{a_1 a_2}{}_a \mathcal{K}^{ea_4}{}_{c,d} - 2\mathcal{K}^{a_3}{}_{eb} \mathcal{K}^{a_1 a_2}{}_a \mathcal{K}^e{}_{fc} \mathcal{K}^{fa_4}{}_d) \delta_{a_1 a_2 a_3 a_4}^{abcd}, \end{aligned}$$

where  $\delta_{a_1 a_2 a_3 a_4}^{abcd} = \epsilon^{abcd} \epsilon_{a_1 a_2 a_3 a_4}$  while the antisymmetric symbol  $\epsilon_{a_1 a_2 a_3 a_4}$  has  $\epsilon_{1234} = 1$  and  $\epsilon^{1234} = -1$ .

Kofinas and Saridakis [5] introduced a different torsion invariant  $T_G$  to formulate a teleparallel equivalent GB term in  $F(T)$  theory. The Gauss-Bonnet term  $\mathcal{G} = R^2 - 4R^{ab}R_{ab} + R^{abcd}R_{abcd}$  in terms of Levi-Civita connection is expressed as

$$h\tilde{\mathcal{G}} = \text{total diverg} + hT_G,$$

where  $h = \det(h_\nu^a)$ . This equation shows that  $T_G$  differs from the GB term only by a total derivative. Also, GB term is not the total derivative. So, the above equation does not imply that  $T_G = 0$ . The action in the context of  $F(T, T_G)$  gravity can be defined as

$$S = \int \sqrt{-g} \left[ \frac{F(T, T_G)}{2\kappa^2} + \mathcal{L}_m \right] d^4x.$$

In the above action,  $\kappa^2 = 1$ ,  $\sqrt{-g} = \det(h_\nu^a)$  with  $h_\nu^a$  represents the tetrad,  $g$  describes the determinant of metric coefficients and  $\mathcal{L}_m$  determines the matter Lagrangian. The basic entity of this theory is tetrad field. The metric tensor and all the terms involve in the action are also expressed in terms of tetrad. So, the field equations can be obtained by varying the action in terms of tetrad field  $h_\nu^a$  as follows

$$\begin{aligned} & \mathcal{C}_{cd}^b (H^{dca} + 2H^{[ac]d}) + (-T_G F_{T_G}(T, T_G) + F(T, T_G) - T F_T(T, T_G)) \eta^{ab} \\ & + 2(H^{[ba]c} - H^{[kcb]a} + H^{[ac]b}) \mathcal{C}_{dc}^d + 2(-H^{[cb]a} + H^{[ac]b} + H^{[ba]c})_{,c} + 4H^{[db]c} \\ & \times \mathcal{C}_{(dc)}^a + T_{cd}^a H^{cdb} - \mathcal{H}^{ab} = \kappa^2 \mathcal{T}^{ab}, \end{aligned} \quad (1)$$

where

$$\begin{aligned} H^{abc} &= (\eta^{ac} K^{bd}_d - K^{bca}) F_T(T, T_G) + F_{T_G}(T, T_G) [(\epsilon^{ab}_{lf} K^{d}_{qr} K^l_{dp} \\ & + 2K^{bc}_p \epsilon^a_{dlf} K^d_{qr} + K^{il}_p \epsilon_{qdlf} K^{jd}_r) K^{qf}_t \epsilon^{kp rt} + \epsilon^{ab}_{ld} K^{fd}_p \epsilon^{cp rt} (K^l_{fr,t} \\ & - \frac{1}{2} \mathcal{C}^q_{tr} K^l_{fq}) + \epsilon^{cp rt} K^{df}_p \epsilon^{al}_{df} (K^b_{kr,t} - \frac{1}{2} \mathcal{C}^q_{tr} K^b_{lq})] + \epsilon^{cp rt} \epsilon^a_{ldf} \\ & \times [F_{T_G}(T, T_G) K^{bl}_{[q} K^{df}_{r]} \mathcal{C}^q_{pt} + (K^{bl}_p F_{T_G}(T, T_G) K^{df}_{r,t})], \\ \mathcal{H}^{ab} &= F_T(T, T_G) \epsilon^a_{lce} K^l_{fr} \epsilon^{br te} K^{fc}_t, \quad F_T(T, T_G) = \frac{d}{dT} F(T, T_G), \\ F_{T_G}(T, T_G) &= \frac{d}{dT_G} F(T, T_G). \end{aligned}$$

Here,  $\mathcal{T}^{ab}$  describes the energy-momentum tensor for matter field. Notice that we can obtain teleparallel equivalent to general relativity (GR) for  $F(T, T_G) = -T$  whereas  $F(T)$  theory is achieved for  $T_G = 0$ .

## 2.2 Wormhole Geometry

A wormhole is known as a hypothetical path like a tunnel or bridge that provides a connection between two different regions of the universe apart from one another. The existence of a realistic wormhole which satisfies the energy conditions has always been a challenging issue. A wormhole through which one can traverse freely is termed as traversable wormhole. The traversability of the wormholes is based on the existence of exotic matter in the wormhole tunnel which violates the NEC. One can easily pass through the tunnel as exotic matter keeps it open but its enough amount give rise to non-realistic wormhole. Hence, the physically viable wormhole solutions exist only if we minimize the amount of this problematic matter in the wormhole throat.

Morris and Thorne [22] were the first who established the notion of traversable wormholes by avoiding event horizon. They proposed a static spherically symmetric metric describing the wormhole geometry [22] as

$$ds^2 = e^{2\lambda(r)} dt^2 - e^{\chi(r)} dr^2 - r^2 d\Omega^2, \quad (2)$$

where  $e^{\chi(r)} = \left(1 - \frac{\psi(r)}{r}\right)^{-1}$  and  $d\Omega^2 = d\theta^2 + \sin^2\theta d\phi^2$ . The above metric entirely depends on two functions, namely redshift function  $\lambda(r)$  and shape function  $\psi(r)$ . The redshift function gives gravitational redshift and shape function determines shape of the wormhole. In order to satisfy the demand of traversable wormhole, we must have small tidal gravitational forces at the throat of the wormhole. For the Schwarzschild wormhole, these forces are so strong that any traveler, who wants to pass through the throat, would be finished. Consequently, the tidal gravitational forces, that affect the traveler, must be sufficiently small.

To avoid event horizon as well as strong tidal forces for a traversable wormhole, we usually assume a non-zero redshift function which is finite everywhere. Hence we assume the function  $\lambda(r)$  as

$$\lambda(r) = -\frac{\zeta}{r}, \quad \zeta > 0, \quad (3)$$

which is non-zero and finite. This satisfies the condition of no horizon as well as asymptotic flatness. To avoid strong tidal forces at throat, we have chosen  $\zeta$  to be small throughout the paper.

For traversable wormhole, the following properties must be satisfied by  $\psi(r)$  and  $\lambda(r)$ .

- The redshift function must fulfill the no horizon property, i.e., it must be finite throughout.
- The asymptotic flatness condition ( $\frac{\psi(r)}{r} \rightarrow 0$  as  $r \rightarrow \infty$ ) should be an essential constituent of the spacetime at large distances.
- The flaring out property ( $\frac{\psi(r)-r\psi'(r)}{\psi^2(r)} > 0$ ) must be satisfied on the wormhole throat radius  $r_{th}$  to obtain an ordinary wormhole solution. Moreover,  $\psi(r)$  satisfies  $\psi'(r_{th}) < 1$  and  $\psi(r) = r_{th}$  at  $r = r_{th}$ .
- The condition  $\left(1 - \frac{\psi(r)}{r}\right) > 0$  must be satisfied at the throat.

To examine the wormhole solutions, we take a diagonal tetrad [22] as

$$h_{\nu}^a = \text{diag} \left( e^{-\lambda(r)}, \left(1 - \frac{\psi(r)}{r}\right)^{-\frac{1}{2}}, r, r \sin \theta \right). \quad (4)$$

This diagonal tetrad is the simplest and frequently used tetrad for the Morris and Thorne static spherically symmetric metric. The expressions for the torsion scalars take the following form

$$T = \frac{2}{r^2} \left(1 - \frac{\psi(r)}{r}\right) + \frac{4\lambda'}{r} \left(1 - \frac{\psi(r)}{r}\right), \quad (5)$$

$$\begin{aligned} T_{\mathcal{G}} &= \frac{8\psi(r)\lambda'(r)}{r^4} - \frac{8\psi(r)\lambda'^2(r)}{r^3} \left(1 - \frac{\psi(r)}{r}\right) + \frac{12\psi(r)\lambda'(r)\psi'(r)}{r^4} \\ &- \frac{8\psi'(r)\lambda'(r)}{r^3} - \frac{12\psi^2(r)\lambda'(r)}{r^5} - \frac{8\psi(r)\lambda''(r)}{r^3} \left(1 - \frac{\psi(r)}{r}\right). \end{aligned} \quad (6)$$

For anisotropic distribution, we assume the following energy-momentum tensor

$$\mathcal{T}_{\mu\nu}^{(m)} = (\rho + p_t)V_{\mu}V_{\nu} - p_t g_{\mu\nu} + (p_r - p_t)\eta_{\mu}\eta_{\nu},$$

where  $V^\mu V_\mu = -\eta^\mu \eta_\mu = 1$  and  $\eta^\mu V_\mu = 0$ ,  $V_\mu$  is the 4-velocity and  $\eta_\mu$  shows the radial spacelike 4-vector which is orthogonal to  $V_\mu$ . We can express the energy-momentum tensor as  $\mathcal{T}_{\mu\nu}^{(m)} = \text{diag}(\rho, -p_r, -p_t, -p_t)$ . Using all the above values in field equations (1), we obtain

$$\begin{aligned} \rho &= F(T, T_G) - TF_T(T, T_G) + \frac{2\psi'(r)}{r^2} F_T(T, T_G) - T_G F_{T_G}(T, T_G) - \frac{4}{r} \left(1 - \frac{\psi(r)}{r}\right) F'_T(T, T_G) + \frac{4}{r^3} \left(\frac{5\psi(r)}{r} - 2 - \frac{3\psi^2(r)}{r^2} - 3\psi'(r) \left(1 - \frac{\psi(r)}{r}\right)\right) \\ &\times F'_{T_G}(T, T_G) + \frac{8}{r^2} \left(1 - \frac{\psi(r)}{r} \left(2 - \frac{\psi(r)}{r}\right)\right) F''_{T_G}(T, T_G), \end{aligned} \quad (7)$$

$$\begin{aligned} p_r &= -F(T, T_G) + \left(T - \frac{2\psi(r)}{r^3} - \frac{4\zeta}{r^3} + \frac{4\psi(r)\zeta}{r^4}\right) F_T(T, T_G) \\ &+ T_G F_{T_G}(T, T_G) + \frac{48\zeta}{r^4} \left(1 - \frac{\psi(r)}{r}\right)^2 F'_{T_G}(T, T_G), \end{aligned} \quad (8)$$

$$\begin{aligned} p_t &= -F(T, T_G) + TF_T(T, T_G) + T_G F_{T_G}(T, T_G) + \left(\frac{\psi(r)}{r^3} - \frac{\psi'(r)}{r^2} - \frac{2\zeta}{r^3}\right. \\ &+ \frac{\psi(r)\zeta}{r^4} + \frac{\psi'(r)\zeta}{r^3} + \frac{2\zeta^2}{r^4} - \frac{2\psi(r)\zeta^2}{r^5} + \frac{4\zeta}{r^3} - \frac{4\psi(r)\zeta}{r^4}\left.) F_T(T, T_G)\right. \\ &+ 2\left(\frac{1}{r} - \frac{\psi(r)}{r^2} - \left(1 - \frac{\psi(r)}{r}\right)\zeta'\right) F'_T(T, T_G) + \left(\frac{12\psi(r)\zeta}{r^5} - \frac{12\psi^2(r)\zeta}{r^6}\right. \\ &+ \frac{12\psi'(r)\zeta}{r^4} + \frac{12\psi(r)\psi'(r)\zeta}{r^5} - \frac{8\zeta^2}{r^5} + \frac{16\psi(r)\zeta^2}{r^6} - \frac{8\psi^2(r)\zeta^2}{r^7} - \frac{16\zeta}{r^4} \\ &- \left.\frac{32\psi(r)\zeta}{r^5} - \frac{16\psi^2(r)\zeta}{r^6}\right) F'_{T_G}(T, T_G) + \left(\frac{8\zeta}{r^3} - \frac{16\psi(r)\zeta}{r^4} + \frac{8\psi^2(r)\zeta}{r^5}\right) \\ &\times F''_{T_G}(T, T_G), \end{aligned} \quad (9)$$

where prime shows derivative with respect to  $r$ . As,  $T_G$  contains quartic torsion terms and it is of the same order with  $T^2$ . Therefore,  $T$  and  $\sqrt{\beta T_G + T^2}$  are of the same order. So, one should use both in a modified theory. The simplest non-trivial  $F(T, T_G)$  model, which does not introduce a new mass scale into the problem and differs from GR, is the one described as [6]

$$F(T, T_G) = \alpha \sqrt{\beta T_G + T^2} - T,$$

where  $\alpha$  and  $\beta$  represent dimensionless non-zero coupling constants. This model represents interesting cosmological behavior and can reveal the new



features of  $F(T, T_G)$  gravity. We have taken the values of  $\alpha$  and  $\beta$  from [6] which provides a detailed analysis of phase space through this model. We choose those values of the parameters that correspond to dark energy dominated era. Also, we take those values of the parameter for which the shape function of Morris and Thorne static spherically symmetric metric satisfies its properties. We cannot fix or bound the values of parameters  $\alpha$  and  $\beta$ . For anisotropic case, we give a detail discussion about the parameters but in the remaining three cases, the properties of the shape function are only satisfied for some particular values of the model that are taken from [6]. Using this model in Eqs.(7)-(9), we obtain complicated form of matter energy density and pressure components given in Appendix **A**.

### 2.3 Energy Conditions

The idea of energy conditions came from Raychaudhuri equations together with the condition of attractive gravity [23]. For timelike  $u^\alpha$  and null  $k^\alpha$  vector field congruences, the Raychaudhuri equations are expressed as follows

$$\begin{aligned}\frac{d\Theta}{d\tau} + R_{\alpha\beta}u^\alpha u^\beta - \omega_{\alpha\beta}\omega^{\alpha\beta} + \sigma_{\alpha\beta}\sigma^{\alpha\beta} + \frac{1}{3}\Theta^2 &= 0, \\ \frac{d\Theta}{d\chi} + R_{\alpha\beta}k^\alpha k^\beta - \omega_{\alpha\beta}\omega^{\alpha\beta} + \sigma_{\alpha\beta}\sigma^{\alpha\beta} + \frac{1}{2}\Theta^2 &= 0,\end{aligned}$$

where  $\omega^{\alpha\beta}$ ,  $\sigma^{\alpha\beta}$  and  $\Theta$  represent the vorticity tensor, shear tensor and expansion scalar, respectively,  $\tau$  and  $\chi$  are the parameters. The expression  $\Theta < 0$  gives the condition of attractive gravity with  $\omega_{\alpha\beta} = 0$  which implies that  $R_{\alpha\beta}u^\alpha u^\beta \geq 0$  and  $R_{\alpha\beta}k^\alpha k^\beta \geq 0$ . In these conditions, the effective energy-momentum tensor is substituted in the place of Ricci tensor, i.e.,  $\mathcal{T}_{\alpha\beta}^{(eff)}u^\alpha u^\beta \geq 0$  and  $\mathcal{T}_{\alpha\beta}^{(eff)}k^\alpha k^\beta \geq 0$  which shows the inclusion of effective energy density and effective pressure in these conditions. The four energy conditions named as NEC, WEC, dominant (DEC) and strong energy condition (SEC) are given as

- NEC:  $p_n^{(eff)} + \rho^{(eff)} \geq 0$ , where  $n = 1, 2, 3$ .
- WEC:  $p_n^{(eff)} + \rho^{(eff)} \geq 0$ ,  $\rho^{(eff)} \geq 0$ ,
- DEC:  $p_n^{(eff)} \pm \rho^{(eff)} \geq 0$ ,  $\rho^{(eff)} \geq 0$ ,
- SEC:  $p_n^{(eff)} + \rho^{(eff)} \geq 0$ ,  $\rho^{(eff)} + 3p^{(eff)} \geq 0$ .

The violation of NEC for  $\mathcal{T}_{\lambda\mu}^{(eff)}$  plays an important role to keep the wormhole throat open and to make it traversable. We evaluate the effective NEC only for radial coordinate from Eqs.(7) and (8) as

$$p_r^{(eff)} + \rho^{(eff)} = \left( \frac{\psi' r - \psi}{r^3} + \frac{2}{r} \left( 1 - \frac{\psi}{r} \right) \lambda' \right).$$

We deduce a condition that shows the violation of effective NEC from the above equation as

$$\left( \frac{\psi' r - \psi}{r^3} + \frac{2}{r} \left( 1 - \frac{\psi}{r} \right) \lambda' \right) < 0. \quad (10)$$

Equation (10) is the necessary condition for the traversability of the wormhole. Thus, the violation of NEC for  $\mathcal{T}_{\alpha\beta}^{(eff)}$  gives a possibility for ordinary matter to fulfil the energy conditions. Hence, the physically acceptable wormhole solutions can be established in this scenario.

### 3 Wormhole Solutions for Various Matter Contents

In this section, we analyze possible solutions by taking four different types of fluid. We examine the validity of traversability condition and also investigate whether  $\mathcal{T}_{\alpha\beta}^m$  satisfies the energy bounds or not.

#### 3.1 Anisotropic Fluid

First, we discuss the anisotropic fluid model by assuming the specific form of  $\chi(r)$  of the metric function as [24]

$$\chi(r) = -\ln \left( 1 - \left( \frac{r_0}{r} \right)^{m+1} \right),$$

where  $r_0$  and  $m$  are arbitrary constants. Since  $e^{\chi(r)} = \left( 1 - \frac{\psi(r)}{r} \right)^{-1}$ , so the shape function becomes

$$\psi(r) = \frac{r_0^{m+1}}{r^m}. \quad (11)$$

It is easy to check that  $\psi(r)$  meets all the conditions necessary to establish

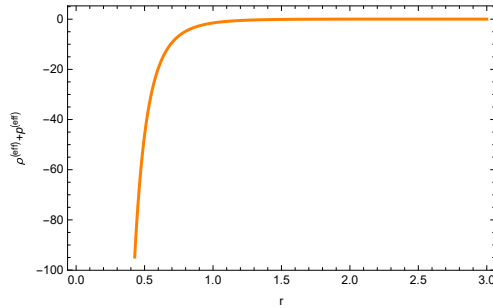


Figure 1: Plot of  $\rho^{(eff)} + p_r^{(eff)}$  versus  $r$  for  $\psi(r) = \frac{r_0^{\frac{3}{2}}}{\sqrt{r}}$ .

a shape function. It satisfies the flaring out condition  $\psi'(r_0) < 1$  for  $m > 1$ ,  $\psi(r_0) = r_0$ . The condition of asymptotically flatness is satisfied for the shape function. Clearly,  $\psi(r)$  is characterized through different values of  $m$  and can provide meaningful results discussed in literature. Lobo and Oliveira [14] assumed the above shape function by choosing  $m = 1, -\frac{1}{2}$  and investigated the wormhole solutions in  $f(R)$  gravity. Pavlovic and Sossich [25] studied the presence of wormholes in the absence of exotic matter by taking  $m = \frac{1}{2}$  in  $f(R)$  gravity.

We take the appropriate parameters involved in the above equations to check the validity of NEC and WEC. We consider different shape functions for  $m = 1/2, 1, -3$ .

- $\psi(r) = \frac{r_0^{\frac{3}{2}}}{\sqrt{r}}$

We discuss effective NEC by substituting the above shape function in Eq.(10) by taking  $m = \frac{1}{2}$ ,  $r_0 = 1$  and  $\zeta = 1$ . In Figure 1, the graphical behavior shows the violation of effective NEC. There appears a possibility for ordinary matter to satisfy the NEC. So, we investigate NEC and WEC for ordinary matter by substituting the above shape function in Eqs.(A1)-(A3). For this purpose, we consider two choices of coupling constant,  $\beta = 1, -1$  with six different values of  $\alpha$ . The behavior of  $\rho + p_r$ ,  $\rho + p_t$  and  $\rho$  is shown in Figure 2. For  $\beta = 1$ , NEC and WEC for ordinary matter are satisfied in the following two regions.

- When  $1.6 \leq r \leq 2.1$ ,  $\alpha_4 = 1$ ,  $\alpha_5 = 2$  and  $\alpha_6 = 3$ , both energy conditions are satisfied for all  $\alpha > 1$ .
- When  $r > 2$ ,  $\alpha_1 = -1$ ,  $\alpha_2 = -2$  and  $\alpha_3 = -3$ , both are valid for all

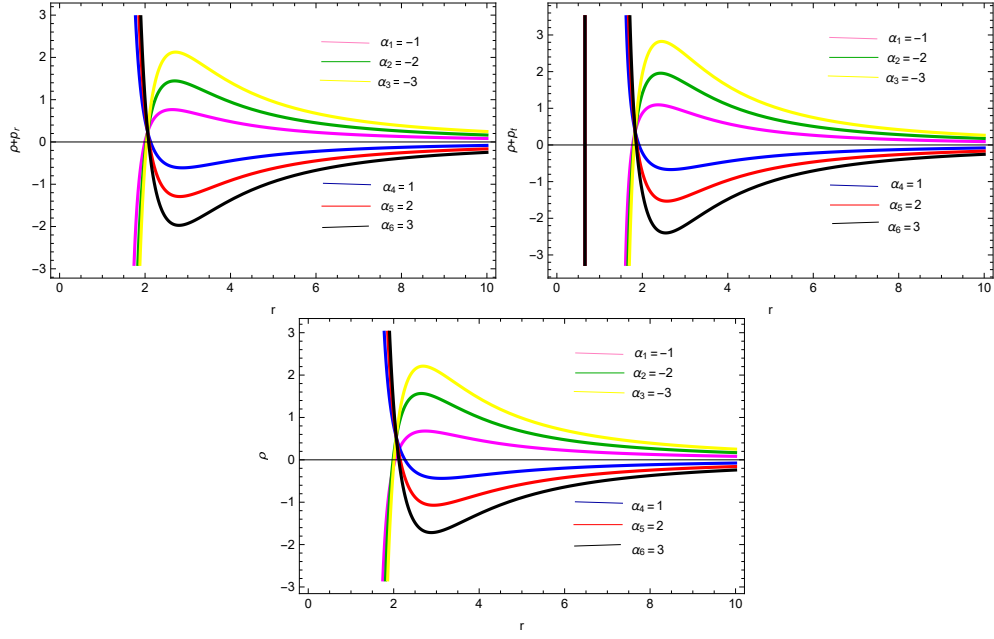


Figure 2: Plots of  $\rho + p_r$ ,  $\rho + p_t$  and  $\rho$  versus  $r$  for  $\beta = 1$ .

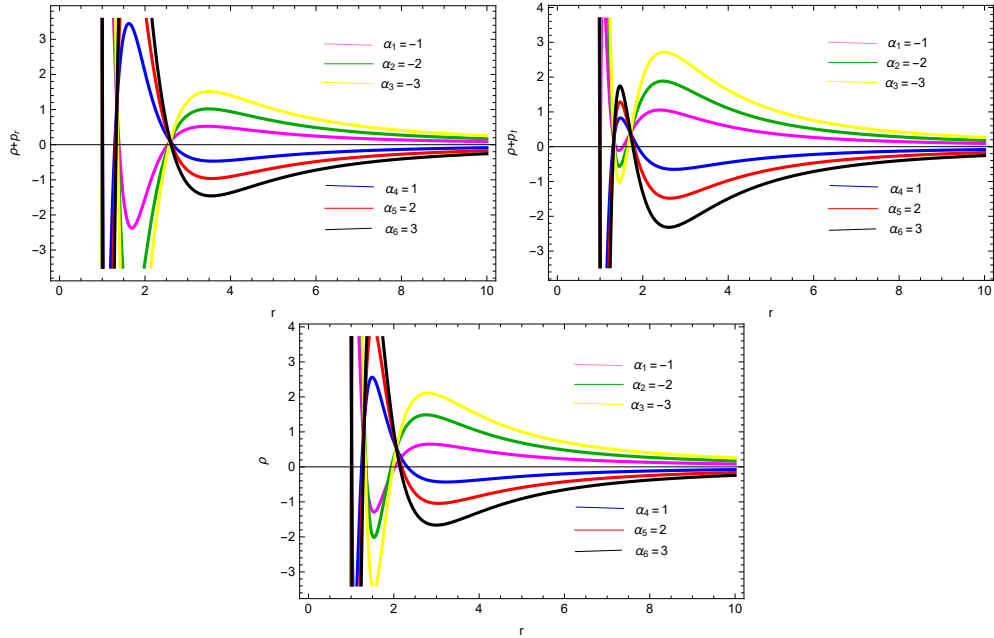


Figure 3: Plots of  $\rho + p_r$ ,  $\rho + p_t$  and  $\rho$  versus  $r$  for  $\beta = -1$ .

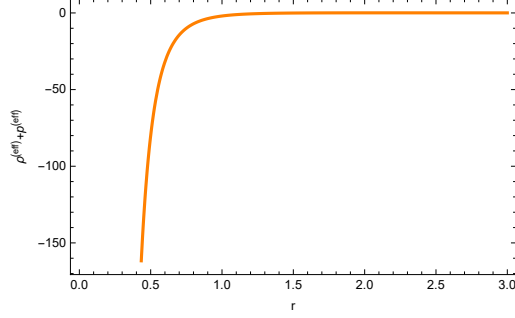


Figure 4: Plot of  $\rho^{(eff)} + p_r^{(eff)}$  versus  $r$  for  $\psi(r) = \frac{r_0^2}{r}$ .

$\alpha < -1$ . In Figure 2, it can be easily seen that  $r$  takes the values in the interval  $1.6 \leq r \leq 10$  for all the six values of  $\alpha$ . Similar results are obtained for all  $\beta > 1$ .

The validity regions of NEC and WEC for  $\beta = -1$  are shown in Figure 3. The positive behavior of  $\rho + p_r$  is obtained in the following three regions.

- (i) When  $1.2 < r < 1.4$  and  $r > 2.7$  for  $\alpha_1 = -1$ ,  $\alpha_2 = -2$  and  $\alpha_3 = -3$ .
- (ii) When  $1.3 < r < 2.7$  for  $\alpha_4 = 1$ ,  $\alpha_5 = 2$  and  $\alpha_6 = 3$ .
- (iii) For  $r = 1$ ,  $\alpha_6 = 3$ .

The positive values of  $\rho + p_t$  can be obtained for the following three ranges of the parameters.

- (i)  $1.1 < r < 1.4$  and  $r > 1.9$  when  $\alpha_1 = -1$ ,  $\alpha_2 = -2$  and  $\alpha_3 = -3$ .
- (ii)  $1.4 < r < 2$  when  $\alpha_4 = 1$ ,  $\alpha_5 = 2$  and  $\alpha_6 = 3$ .
- (iii) For  $r = 1$ ,  $\alpha_6 = 3$ .

Finally,  $\rho > 0$  is satisfied for the following three cases.

- (i)  $1.1 < r < 1.4$  and  $r > 1.9$  for  $\alpha_1 = -1$ ,  $\alpha_2 = -2$  and  $\alpha_3 = -3$ .
- (ii)  $1.4 < r < 2.2$  for  $\alpha_4 = 1$ ,  $\alpha_5 = 2$  and  $\alpha_6 = 3$ .
- (iii) For  $r = 1$ ,  $\alpha_6 = 3$ .

Thus, the following validity regions for both energy conditions (NEC and WEC) are

- (i)  $1.3 < r < 1.4$  and  $r > 2$  when  $\alpha_1 = -1$ ,  $\alpha_2 = -2$ ,  $\alpha_3 = -3$ .
- (ii)  $1.4 < r < 2.1$  when  $\alpha_4 = 1$ ,  $\alpha_5 = 2$  and  $\alpha_6 = 3$ .
- (iii) For  $r = 1$ ,  $\alpha_6 = 3$ .

The validity of NEC and WEC for ordinary leads to similar results for all  $\beta < -1$ ,  $\alpha < -1$ ,  $\alpha > 1$ . Thus, there exist physically acceptable wormholes in the above mentioned regions.

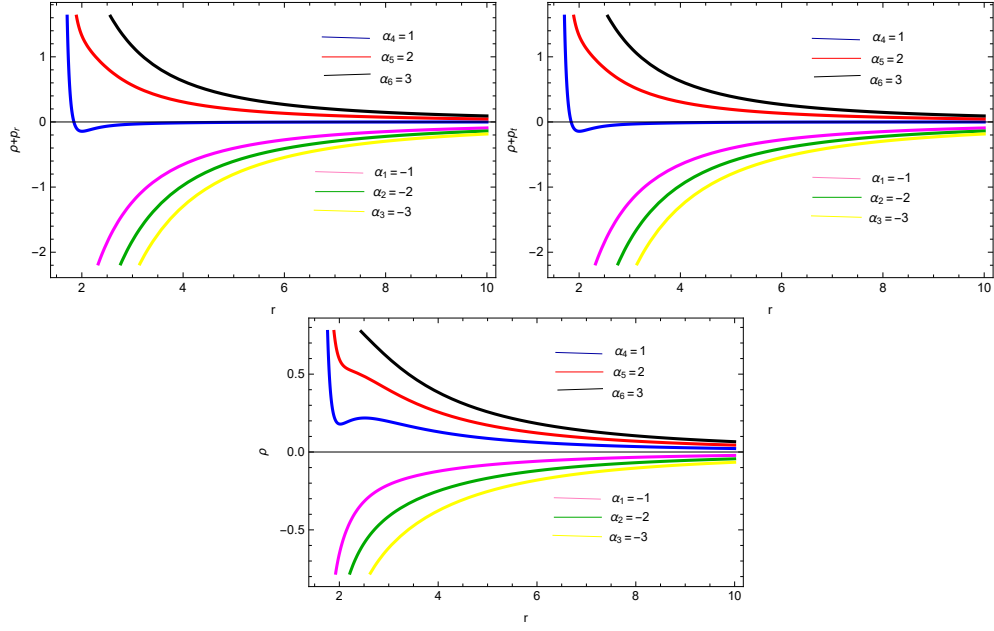


Figure 5: Plots of  $\rho + p_r$ ,  $\rho + p_t$  and  $\rho$  versus  $r$  for  $\beta = 1$ .

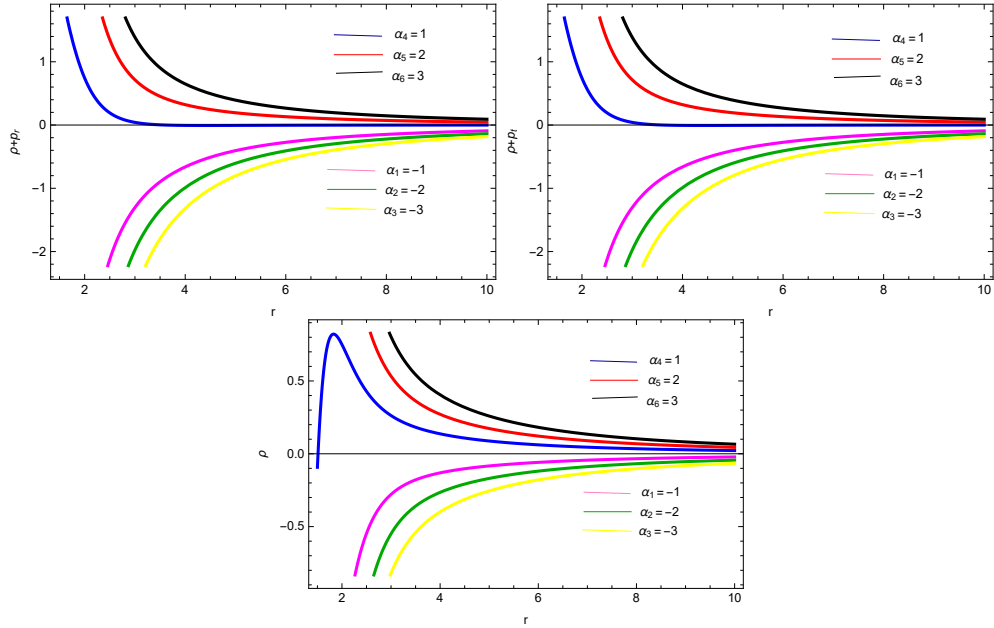


Figure 6: Plots of  $\rho + p_r$ ,  $\rho + p_t$  and  $\rho$  versus  $r$  for  $\beta = -1$ .

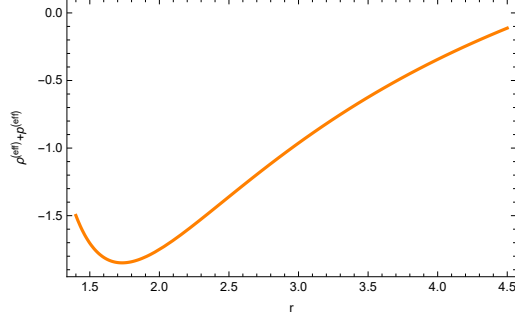


Figure 7: Plot of  $\rho^{(eff)} + p_r^{(eff)}$  versus  $r$  for  $\psi(r) = \frac{r^3}{r_0^2}$ .

- $\psi(r) = \frac{r_0^2}{r}$ .

For  $m = 1$ , we obtain the above shape function. We check the condition of traversability given in (10). In Figure 4,  $\rho^{(eff)} + p_r^{(eff)}$  shows negative behavior versus  $r$  that confirms the validity of condition (10). We also investigate the NEC as well as WEC for ordinary matter. For this purpose, we use the above value of shape function in Eqs.(A1)-(A3) and find the corresponding results for  $\rho + p_r$ ,  $\rho + p_t$  and  $\rho$ . We discuss these results by choosing the parametric values  $\zeta = 1$  and  $r_0 = 1$ . Figure 5 shows that both  $\rho + p_r$  and  $\rho + p_t$  represent positive behavior in the intervals  $1.9 < r < 10$  for  $\alpha_5 = 2$  and  $2.5 < r < 10$  for  $\alpha_6 = 3$ . Also,  $\rho + p_r$  and  $\rho + p_t$  show negatively increasing behavior for negative values of  $\alpha$ . The energy density indicates positively decreasing behavior for  $\alpha_4 = 1$ ,  $\alpha_5 = 2$ ,  $\alpha_6 = 3$  and negatively decreasing behavior for  $\alpha_1 = -1$ ,  $\alpha_2 = -2$ ,  $\alpha_3 = -3$ . Thus for  $\beta = 1$ , NEC and WEC hold in the following regions: (i)  $1.9 < r < 10$ ,  $2.5 < r < 10$  when  $\alpha_5 = 2$  and  $\alpha_6 = 3$ . (ii)  $1.6 < r < 1.8$  for  $\alpha_4 = 1$ . When  $\beta = -1$ , the graphical results of  $\rho + p_r$ ,  $\rho + p_t$  and  $\rho$  are shown in Figure 6. We can observe that for all  $\alpha > 1$ , the plots of  $\rho + p_r$ ,  $\rho + p_t$  and  $\rho$  satisfy NEC and WEC. For all  $\alpha < -1$ , the behavior of  $\rho + p_r$ ,  $\rho + p_t$  and  $\rho$  do not meet the energy conditions.

- $\psi(r) = \frac{r^3}{r_0^2}$ .

Here, we set  $m = -3$  to have the above shape function. The graph of  $\rho^{(eff)} + p_r^{(eff)}$  is shown in Figure 7. It can be observed that the effective NEC does not hold for  $m = -3$ . We check the behavior of NEC and WEC for ordinary matter. The corresponding values of  $\rho + p_r$ ,  $\rho + p_t$  and  $\rho$  are

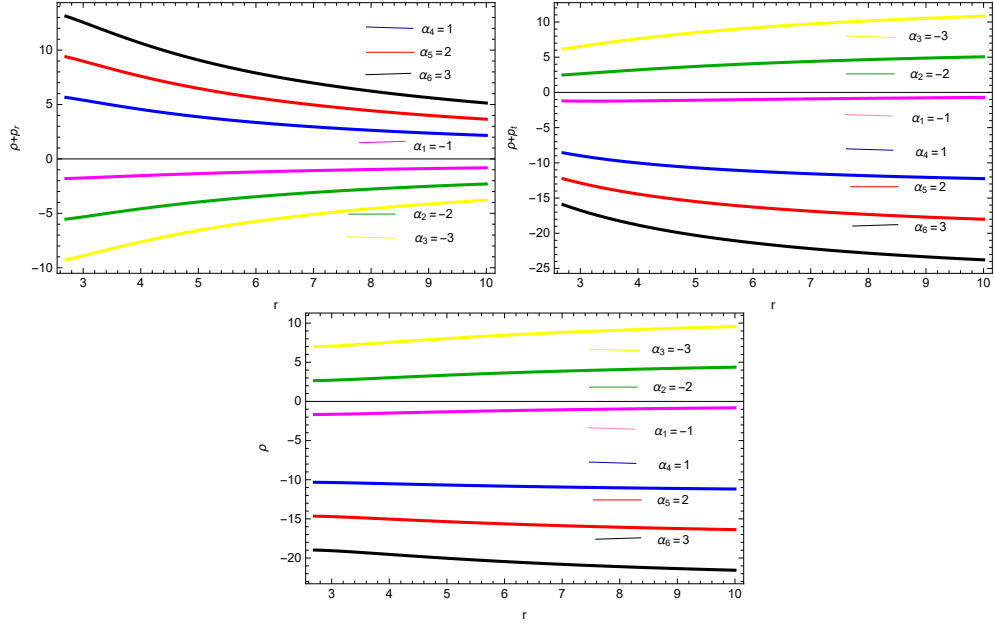


Figure 8: Plots of  $\rho + p_r$ ,  $\rho + p_t$  and  $\rho$  versus  $r$  for  $\beta = 1$ .

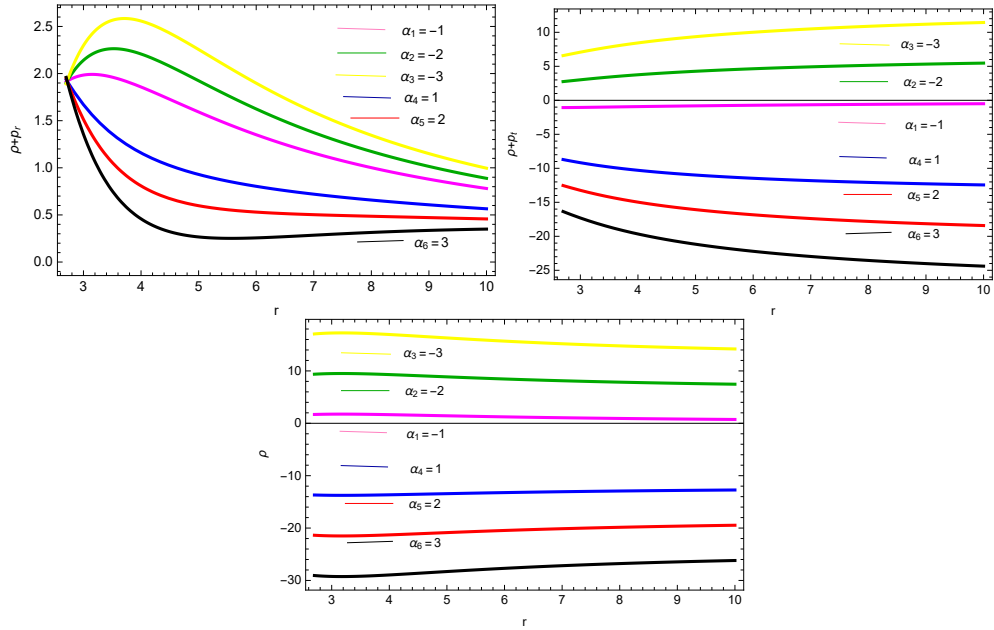


Figure 9: Plots of  $\rho + p_r$ ,  $\rho + p_t$  and  $\rho$  versus  $r$  for  $\beta = -1$ .



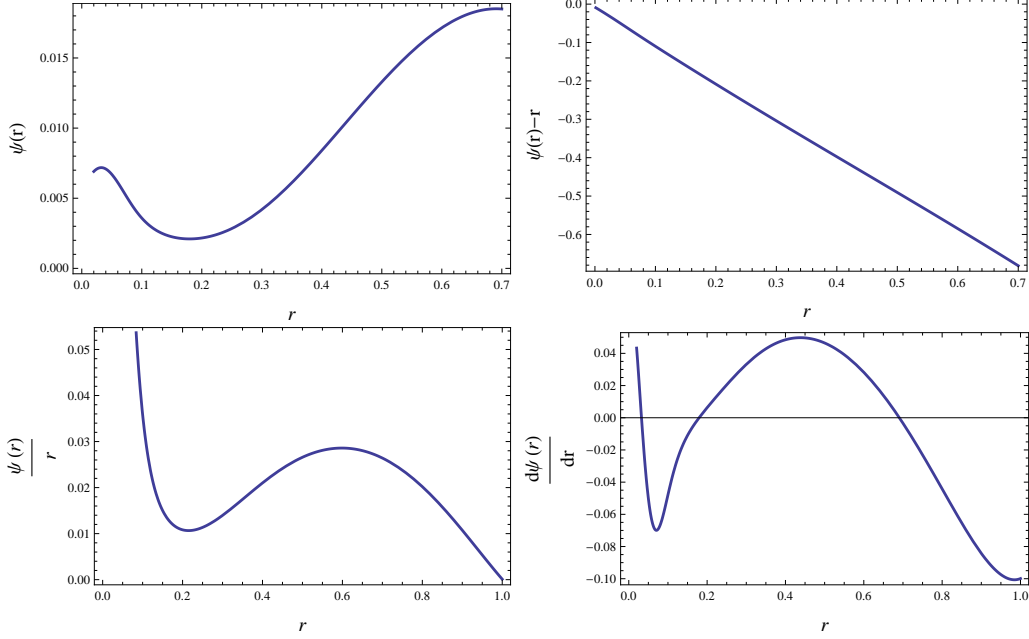


Figure 10: Plots of  $\psi(r)$ ,  $\psi(r) - r$ ,  $\frac{\psi(r)}{r}$  and  $\frac{d\psi(r)}{dr}$  versus  $r$  for isotropic case.

shown in Figure 8. We discuss their behavior by choosing different values of the parameters  $\alpha$ ,  $\beta$  and  $r$ . For  $\beta = 1$ , we see that  $\rho + p_r > 0$  for  $r \geq 2.7$ ,  $\alpha_4 = 1$ ,  $\alpha_5 = 2$  and  $\alpha_6 = 3$ , i.e., for all  $\alpha > 1$ . We find that  $\rho + p_t > 0$  and  $\rho > 0$  for  $r \geq 2.7$ ,  $\alpha_2 = -2$  and  $\alpha_3 = -3$ . We also check that their values remain positive for all  $\alpha > -1.5$ . There is no similar region between  $\rho + p_r$  and  $\rho + p_t$ , hence NEC and WEC do not hold for ordinary matter. For  $\beta = -1$ , both energy conditions are valid if  $r > 2.7$  and  $\alpha > -2$  as shown in Figure 9. Similar results hold for all  $\beta < -1$ . Thus, there exists a realistic wormhole for  $r > 2.7$  and for all  $\alpha > -2$  and  $\beta < -1$ .

### 3.2 Isotropic Fluid

The equation for isotropic fluid ( $p = p_r = p_t$ ) is obtained from Eqs.(A2) and (A3) given in Appendix A.

This equation is highly nonlinear which cannot be solved analytically. We discuss the behavior of shape function and energy conditions numerically to analyze wormhole solutions for  $\zeta = 0.1$ ,  $\alpha = -2$  and  $\beta = 10$ . Figure 10 shows that  $\psi(r)$  represents the increasing behavior in the interval  $0.2 \leq r \leq 0.7$

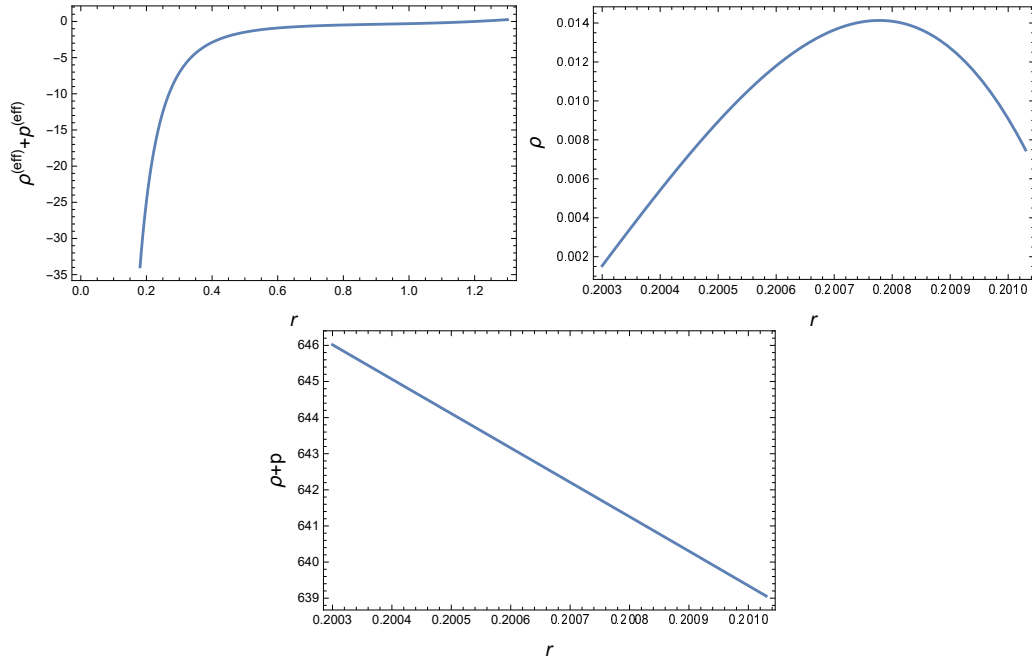


Figure 11: Plots of  $\rho^{(eff)} + p_r^{(eff)}$ ,  $\rho$  and  $\rho + p$  versus  $r$  for isotropic case.

and satisfies the condition  $\psi(r) < r$ . We find throat of the wormhole at  $r_{th} = 0.004$  as  $\psi(0.004) = 0.00366$ . The asymptotic flatness condition is also satisfied. The plot of the derivative of shape function indicates that  $\frac{d\psi(r_{rh})}{dr} < 1$ .

The upper left panel of Figure 11 shows the violating behavior of effective NEC. The upper right panel and lowerpanel of Figure 11 represents the evolution of  $\rho$  and  $\rho + p$  versus  $r$ . The energy density and for ordinary matter shows positive behavior in the interval  $0.2003 \leq r \leq 0.2010$ . In the right plot of Figure 12,  $\rho + p$  lies totally in the positive region for the same range of  $r$ . Hence, there may exist a region of similarity between the two graphs. This shows that both NEC and WEC satisfy for the isotropic fluid. Hence, there exists a realistic wormhole in the interval  $0.2003 \leq r \leq 0.2010$  for  $\alpha = -2$  and  $\beta = 10$ .

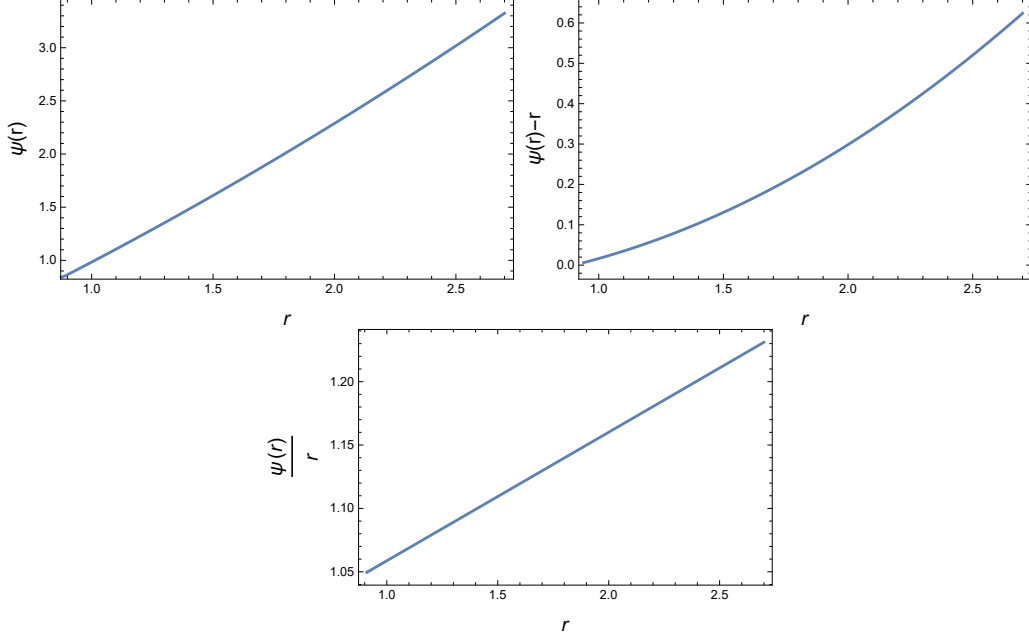


Figure 12: Plots of  $\psi(r)$ ,  $\psi(r) - r$  and  $\frac{\psi(r)}{r}$  versus  $r$  for barotropic case.

### 3.3 Barotropic Equation of State

We assume an equation of state which involves energy density and radial pressure, i.e.,  $\mu\rho = p_r$ , where  $\mu$  is the equation of state parameter. This specific equation of state has been studied in literature to examine the wormhole solutions [15, 19, 24]. The equation for barotropic fluid is obtained from Eqs.(A1) and (A2) given in Appendix **A**. We solve the above equation numerically to obtain the value of  $\psi(r)$  with  $m = \frac{1}{2}$ ,  $\zeta = 0.1$ ,  $\alpha = 2$ ,  $\mu = 0.001$  and  $\beta = 2$ . The left panel of Figure **12** shows that  $\psi(r)$  increases as the value of  $r$  increases. The wormhole throat is found at very small values of  $r$ . Also, the plot of  $\frac{\psi(r)}{r}$  shows that the spacetime is not asymptotically flat. The upper left panel of Figure **13** represents the violation of effective NEC. We investigate the behavior of NEC/WEC for ordinary matter. In Figure **13**, it can be observed that  $\rho$ ,  $\rho + p_r$  and  $\rho + p_t$  exhibit negative values. Thus, there does not exist realistic wormhole and wormhole geometries are maintained through exotic matter.

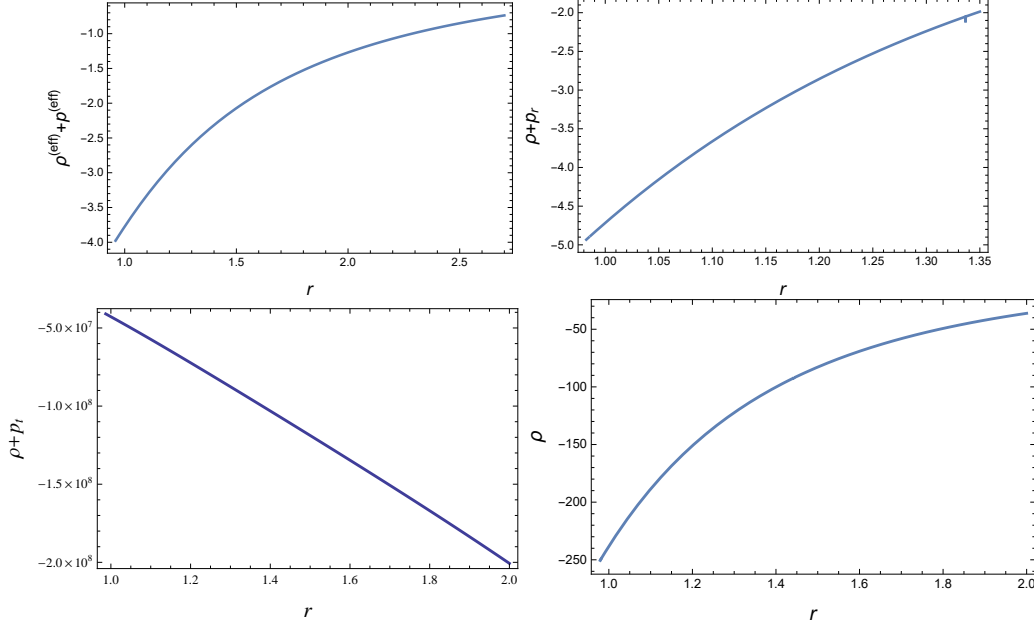


Figure 13: Plots of  $\rho^{(eff)} + p_r^{(eff)}$ ,  $\rho + p_r$ ,  $\rho + p_t$  and  $\rho$  versus  $r$  for barotropic case.

### 3.4 Traceless Fluid

In this case, we investigate the wormhole solutions through an interesting equation of state for traceless fluid, i.e.,  $2p_t - \rho + p_r = 0$  [14, 15]. Therefore, Eqs.(A1)-(A3) reduce to the equation given in Appendix **A**. Here, we consider the following parameters  $m = \frac{1}{2}$ ,  $\zeta = 0.1$ ,  $\alpha = -2$  and  $\beta = -2$ . Figure 14 shows the increasing behavior of  $\psi(r)$  and the plot of  $\psi(r) - r$  locates throat of the wormhole at very small values of  $r$ . The plot of  $\frac{\psi(r)}{r}$  indicates that the spacetime is asymptotically flat. The derivative of  $\psi(r)$  satisfies  $\psi'(r_{th}) < 1$ . The upper left panel of Figure 15 indicates the validity of condition (10). The graphs of  $\rho + p_r$ ,  $\rho + p_t$  and  $\rho$  (for ordinary matter) express positive values in the interval  $0.06 < r < 0.2$  as shown in Figure 15. Thus NEC as well as WEC are satisfied for normal matter in this case. This shows that physically acceptable wormhole exists in this case for  $\alpha$  and  $\beta$  is equal to  $-2$ .

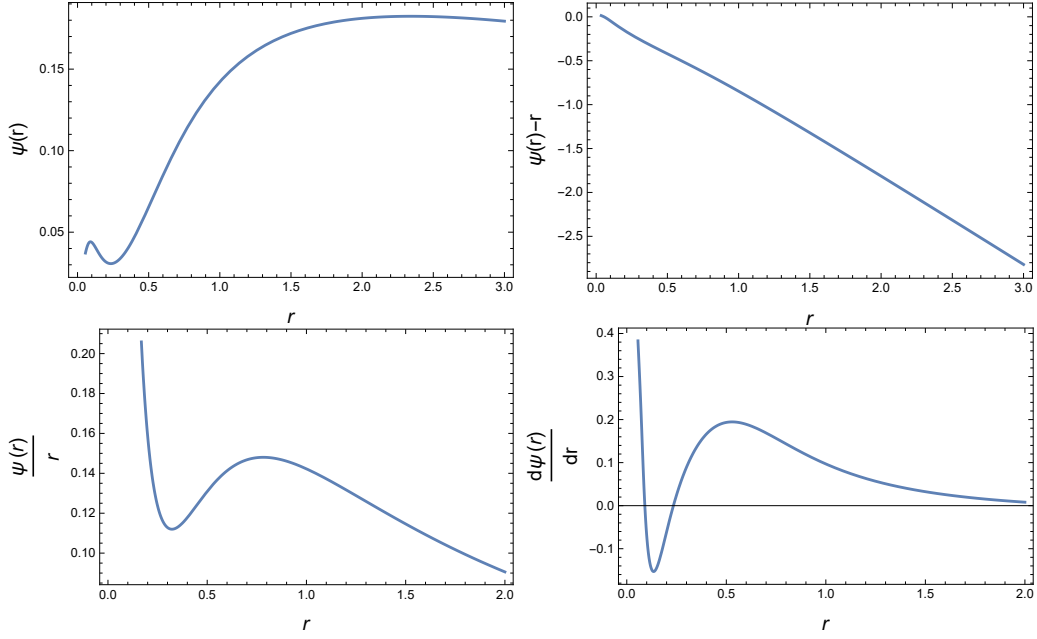


Figure 14: Plots of  $\psi(r)$ ,  $\psi(r) - r$ ,  $\frac{\psi(r)}{r}$  and  $\frac{d\psi(r)}{dr}$  versus  $r$  for traceless case.

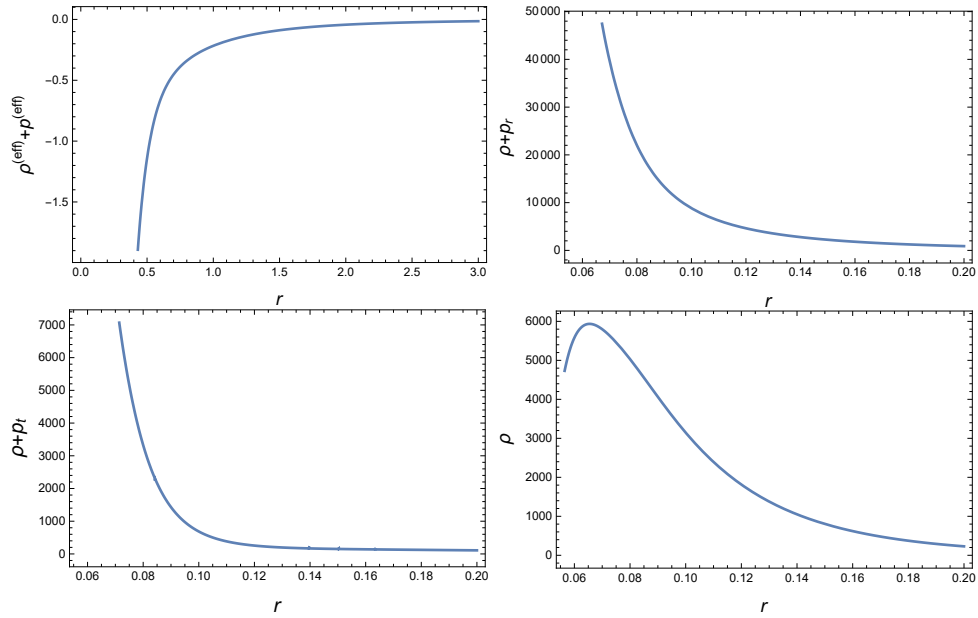


Figure 15: Plots of  $\rho^{(eff)} + p_r^{(eff)}$ ,  $\rho + p_r$ ,  $\rho + p_t$  and  $\rho$  versus  $r$  for traceless case.

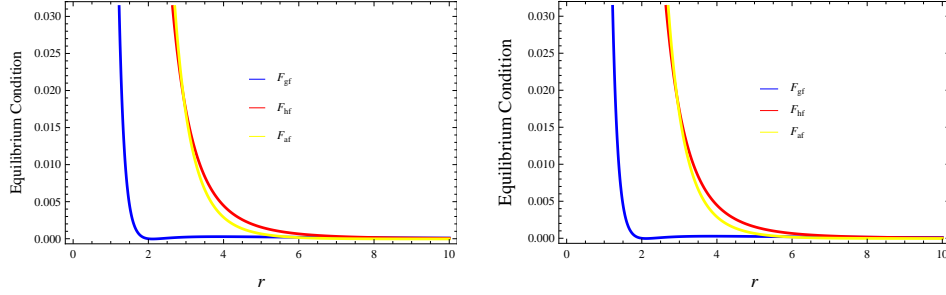


Figure 16: Plot of three different forces  $F_{gf}$ ,  $F_{hf}$  and  $F_{af}$  versus  $r$  for  $\beta = 1$  and  $\beta = -1$ .

## 4 Equilibrium Condition

Here, we study stability of static wormhole solutions by analyzing the equilibrium configuration. For this purpose, we deal with the generalized form of Tolman–Oppenheimer–Volkov (TOV) equation in an effective manner given as

$$(p_t^{(eff)} - p_r^{(eff)}) \left( \frac{2}{r} \right) - (p_r^{(eff)} + \rho^{(eff)}) \left( \frac{\chi'(r)}{2} \right) - p_r'^{(eff)} = 0.$$

We rewrite the above equation as

$$- (p_r^{(eff)} + \rho^{(eff)}) \left( \frac{M^{(eff)} e^{\frac{\lambda-\chi}{2}}}{r^2} \right) + (p_t^{(eff)} - p_r^{(eff)}) \left( \frac{2}{r} \right) - p_r'^{(eff)} = 0, \quad (12)$$

where  $M^{(eff)} = \frac{1}{2} \left( r^2 e^{\frac{\lambda-\chi}{2}} \right) \chi'$  is the effective gravitational mass. This equation provides the equilibrium picture of static wormhole solutions through three forces namely gravitational force  $F_{gf}$ , anisotropic force  $F_{af}$  and hydrostatic force  $F_{hf}$ . The gravitational force appears as the result of gravitating mass, anisotropic force arises due to anisotropy of the system and hydrostatic force occurs as a result of hydrostatic fluid. We can rewrite Eq.(12) as

$$F_{af} + F_{gf} + F_{hf} = 0, \quad (13)$$

where

$$F_{af} = (p_t^{(eff)} - p_r^{(eff)}) \left( \frac{2}{r} \right), F_{gf} = - (p_r^{(eff)} + \rho^{(eff)}) \left( \frac{\chi'(r)}{2} \right),$$

$$F_{hf} = -\frac{dp_r^{(eff)}}{dr}.$$

Using Eqs.(A1)-(A3) in (13), we obtain an equation which is solved by applying numerical scheme for  $m = \frac{1}{2}$ ,  $\alpha = -0.0009$  and  $\zeta = 0.1$ . The graphs of three different forces are shown in Figure **16** for  $\beta = 1$  (left panel) and  $\beta = -1$  (right panel), respectively. In both plots, we see that the net result of three forces is zero for  $r > 6$ . Hence the wormhole solutions balance the system implying that these solutions are stable.

## 5 Final Remarks

In general relativity, the existence of static and traversable wormholes depends on the presence of exotic matter that violates the energy conditions. On the other hand, the status may be totally different in modified theories. In this paper, we have explored the existence of static and traversable wormhole solutions in the context of  $F(T, T_{\mathcal{G}})$  gravity for a particular model using four types of matter contents. For anisotropic case, we have assumed a shape function to discuss the validity of energy conditions while for the remaining three cases (isotropic, barotropic and traceless), we have evaluated the shape function and studied the energy conditions.

For anisotropic fluid, we have explored energy constraints by using two values of coupling constant  $\beta = 1$  and  $\beta = -1$ . We have checked the effective NEC for  $m = \frac{1}{2}, 1$  and  $-3$ . We have observed that this condition violates for all the three values of  $m$ . This violation provides a chance to normal matter to satisfy the NEC. The energy conditions for normal matter are satisfied for positive values of  $\alpha$  in the specific regions for both  $\beta = 1, -1$ . We have also checked NEC and WEC for  $\beta > 1$  and  $\beta < -1$  and obtained similar results. We have discussed three shape functions with their energy constraints and found results consistent for  $m = -3$  [21]. For the other three fluids, we have analyzed solutions numerically to explain the structure of the shape function and to check the validity of NEC and WEC.

For isotropic and traceless fluids, all the basic requirements are satisfied by the shape function. The condition for effective NEC is also satisfied in each case which confirms the presence of traversable wormhole. The energy conditions for ordinary matter are also verified for these two fluids. Thus, there exist physically acceptable wormhole solutions for these fluids. In the barotropic case, the shape function is not asymptotically flat. The condition

for effective NEC is satisfied but energy conditions for ordinary matter are violated. Hence, no realistic wormhole solution is found for barotropic case. We have also explored stability of the wormhole solutions with anisotropic fluid. It is found that the equilibrium condition holds and wormhole solutions are stable. We can conclude that the effective energy-momentum tensor plays a significant role to violate the energy conditions in  $F(T, T_G)$  gravity. This violation guarantees the presence of traversable wormhole solutions.

## Appendix A

The values of matter energy density and pressure components are

$$\begin{aligned}
\rho &= -Y + \alpha(Y^2 + \beta X)^{\frac{1}{2}} - Y(-1 + (\alpha Y)/(Y^2 + \beta X)^{\frac{1}{2}}) - \frac{1}{2}(X\alpha\beta)/ \\
&\times (Y^2 + \beta X)^{\frac{1}{2}} + \frac{1}{r^2}(2\psi'(r)(-1 + (\alpha Y)/(Y^2 + \beta X)^{\frac{1}{2}})) - \frac{1}{r}(4(1 \\
&- \frac{\psi(r)}{r})(-(\alpha Y^2)/(Y^2 + \beta Y)^{\frac{3}{2}} + \alpha/(Y^2 + \beta X)^{\frac{1}{2}}) \left( -\frac{9}{r^4} \left( 1 - \frac{\psi(r)}{r} \right) \right. \\
&\times \left. \zeta + \frac{3}{r^3} \left( -\frac{\psi'(r)}{r} + \frac{\psi(r)}{r^2} \right) \zeta - \frac{8}{r^5} \left( 1 - \frac{\psi(r)}{r} \right) \zeta + \frac{2}{r^4} \left( -\frac{\psi'(r)}{r} \right. \right. \\
&+ \left. \left. \frac{\psi(r)}{r^2} \right) \zeta - \frac{4}{r^3} \left( 1 - \frac{\psi(r)}{r} \right) + \frac{2}{r^2} \left( -\frac{\psi'(r)}{r} + \frac{\psi(r)}{r^2} \right) \right) - \left( \left( 5\frac{\psi(r)}{r} - 2 \right. \right. \\
&- \left. \left. 3\frac{\psi(r)^2}{r^2} - 3\psi'(r)\left(1 - \frac{\psi(r)}{r}\right)\right)\alpha\beta^2 \left( \frac{12\zeta\psi'^2(r)}{r^6} + \frac{12\zeta\psi(r)\psi''(r)}{r^6} \right. \right. \\
&- \left. \frac{128\zeta\psi(r)\psi'(r)}{r^7} - \frac{8\zeta^2\psi(r)}{r^7} + \frac{56\zeta^2\psi(r)}{r^8} + \frac{196\zeta\psi^2(r)}{r^8} + \frac{12\zeta\psi'(r)}{r^7} \right. \\
&- \left. \left. \frac{84\zeta\psi(r)}{r^8} - \frac{8\zeta\psi''(r)}{r^5} + \frac{40\zeta\psi'(r)}{r^6} + \frac{16\zeta^2\psi(r)\psi'(r)}{r^8} - \frac{64\zeta^2\psi^2(r)}{r^9} \right) \right) \\
&\left( r^3(Y^2 + \beta X)^{\frac{3}{2}} + \frac{1}{r^2}\left(8\left(1 - \frac{\psi(r)}{r}\right)\left(2 - \frac{\psi(r)}{r}\right)\right)\right)\left(\frac{3}{8}(\alpha\beta^3 \left( \frac{12\zeta\psi'^2(r)}{r^6} \right. \right. \right. \\
&+ \left. \left. \frac{12\zeta\psi(r)\psi''(r)}{r^6} - \frac{128\zeta\psi(r)\psi'(r)}{r^7} - \frac{8\zeta^2\psi(r)}{r^7} + \frac{56\zeta^2\psi(r)}{r^8} + \frac{196\zeta\psi^2(r)}{r^8} \right. \right. \\
&+ \left. \left. \frac{12\zeta\psi'(r)}{r^7} - \frac{84\zeta\psi(r)}{r^8} - \frac{8\zeta\psi''(r)}{r^5} + \frac{40\zeta\psi'(r)}{r^6} + \frac{16\zeta^2\psi(r)\psi'(r)}{r^8} \right) \right)
\end{aligned}$$



$$\begin{aligned}
& - \frac{64\zeta^2\psi^2(r)}{r^9} \Big)^2 \Big) / (Y^2 + \beta X) \frac{5}{2} - \frac{1}{4} (\alpha\beta^2 (-\frac{240\zeta\psi'(r)}{r^7} + \frac{12\zeta\psi''(r)}{r^7} \\
& - \frac{8\zeta\psi'''(r)}{r^5} - \frac{8\zeta^2\psi''(r)}{r^7} - \frac{200\zeta\psi(r)\psi''(r)}{r^7} + \frac{1288\zeta\psi(r)\psi'(r)}{r^8} \\
& - \frac{256\zeta^2\psi(r)\psi'(r)}{r^9} + \frac{576\zeta^2\psi^2(r)}{r^{10}} + \frac{36\zeta\psi'(r)\psi''(r)}{r^6} - \frac{200\zeta\psi'(r)}{r^7} \\
& + \frac{12\zeta\psi(r)\psi'''(r)}{r^6} + \frac{112\zeta^2\psi'(r)}{r^8} - \frac{448\zeta^2\psi(r)}{r^9} - \frac{1568\zeta\psi^2(r)}{r^9} \\
& - \frac{168\zeta\psi'(r)}{r^8} + \frac{672\zeta\psi(r)}{r^9} + \frac{80\zeta\psi''(r)}{r^6} + \frac{16\zeta^2\psi'^2(r)}{r^8} + \frac{16\zeta^2\psi(r)\psi''(r)}{r^8} \Big) \\
& / (Y^2 + \beta X^{\frac{3}{2}}), \tag{A1}
\end{aligned}$$

$$\begin{aligned}
p_r &= Y - \alpha(Y^2 + \beta X)^{\frac{1}{2}} + \left(\frac{2}{r^2}\left(1 - \frac{2\psi(r)}{r}\right) + \frac{4}{r^3}\left(1 - \frac{2\psi(r)}{r}\right)\zeta\right)(-1 + (\alpha \\
& \times Y)/(Y^2 + \beta X)^{\frac{1}{2}} + \frac{1}{2}\left(\left(\frac{12\zeta\psi(r)\psi'(r)}{r^6} - \frac{8\zeta^2\psi(r)}{r^7} - \frac{28\zeta\psi^2(r)}{r^7}\right. \right. \\
& + \left.\left.\frac{12\zeta\psi(r)}{r^7} - \frac{8\zeta\psi'(r)}{r^5} + \frac{8\zeta^2\psi^2(r)}{r^8}\right)\alpha\beta\right)/(Y^2 + \beta X)^{\frac{1}{2}} + (6\zeta(1 \\
& - \frac{2\psi(r)}{r})^2\alpha\beta^2\left(\frac{12\zeta\psi'^2(r)}{r^6} + \frac{12\zeta\psi'(r)}{r^7} - \frac{12\zeta\psi(r)}{r^8} - \frac{8\zeta\psi''(r)}{r^5} + \frac{40\zeta\psi'(r)}{r^6}\right. \\
& + \left.\frac{16\zeta^2\psi'(r)}{r^8} - \frac{64\zeta^2\psi^2(r)}{r^9}\right))/(r^4(Y^2 + \beta X)^{\frac{3}{2}}), \tag{A2}
\end{aligned}$$

$$\begin{aligned}
p_t &= Y - \alpha(Y^2 + \beta X)^{\frac{1}{2}} + \left(\frac{1}{r}\left(2 - \frac{\psi(r)}{r} - \frac{\psi'(r)}{r}\right)\left(\frac{\zeta}{r^2} + \frac{1}{r}\right) + 2\left(1 - \frac{\psi(r)}{r}\right) \right. \\
& \times \left.\left(\frac{\zeta^2}{r^4} - \frac{2\zeta}{r^3}\right)\right)(-1 + (\alpha Y)/(Y^2 + \beta X)^{\frac{1}{2}}) + \frac{1}{2}(X\alpha\beta)/(Y^2 + \beta X)^{\frac{1}{2}} \\
& + 2\left(1 - \frac{\psi(r)}{r}\right)\left(\frac{\zeta}{r^2} + \frac{1}{r}\right)(-\alpha Y^2)/(Y^2 + \beta X)^{\frac{3}{2}} + \alpha/(Y^2 + \beta X)^{\frac{1}{2}} \\
& \times \left(-\frac{9}{r^4}\left(1 - \frac{\psi(r)}{r}\right)\zeta + \frac{3}{r^3}\left(-\frac{\psi'(r)}{r} + \frac{\psi(r)}{r^2}\right)\zeta - \frac{8}{r^5}\left(1 - \frac{\psi(r)}{r}\right)\zeta + \frac{2}{r^4}\left(-\frac{\psi'(r)}{r} \right. \right. \\
& + \left.\left.\frac{\psi(r)}{r^2}\right)\zeta - \frac{4}{r^3}\left(1 - \frac{\psi(r)}{r}\right) + \frac{2}{r^2}\left(-\frac{\psi'(r)}{r} + \frac{\psi(r)}{r^2}\right)\right) - \frac{1}{4}\left(\left(\frac{12\zeta}{r^4}(\psi'(r) + \frac{\psi(r)}{r^2})\right. \right. \\
& - \left.\left.\frac{8}{r}\left(\frac{\zeta^2}{r^4} - \frac{2\zeta}{r^3}\right)\left(1 - \frac{\psi(r)}{r}\right)^2\right)\alpha\beta^2\left(\frac{12\zeta\psi'^2(r)}{r^6} + \frac{12\zeta\psi(r)\psi''(r)}{r^6}\right. \right. \\
& + \left.\left.\frac{56\zeta^2\psi(r)}{r^8} - \frac{8\zeta^2\psi(r)}{r^7} - \frac{128\zeta\psi(r)\psi'(r)}{r^7} + \frac{196\zeta\psi^2(r)}{r^8} + \frac{12\zeta\psi'(r)}{r^7}\right) \right)
\end{aligned}$$

$$\begin{aligned}
& - \left. \left( \frac{84\zeta\psi(r)}{r^8} + \frac{8\zeta\psi''(r)}{r^5} + \frac{40\zeta\psi'(r)}{r^6} + \frac{16\zeta^2\psi(r)\psi'(r)}{r^8} - \frac{64\xi^2\psi^2(r)}{r^9} \right) \right) \\
& / \left( Y^2 + \beta X \right)^{\frac{3}{2}} - \frac{1}{r^3} \left( 8\xi \left( 1 - \frac{\psi(r)}{r} \right) \right)^2 \left( \frac{3}{8} (\alpha\beta^3 \left( \frac{12\zeta\psi'^2(r)}{r^6} + \frac{12\zeta\psi'(r)}{r^7} \right. \right. \right. \\
& - \frac{128\zeta\psi(r)\psi'(r)}{r^7} + \frac{12\zeta\psi(r)\psi''(r)}{r^6} - \frac{8\zeta^2\psi(r)}{r^7} + \frac{56\zeta^2\psi(r)}{r^8} \\
& + \frac{196\zeta\psi^2(r)}{r^8} - \frac{84\zeta\psi(r)}{r^8} - \frac{8\zeta\psi''(r)}{r^5} + \frac{40\zeta\psi'(r)}{r^6} + \frac{16\zeta^2\psi(r)\psi'(r)}{r^8} \\
& \left. \left. \left. - \frac{64\zeta^2\psi^2(r)}{r^9} \right)^2 \right) / (Y^2 + \beta X)^{\frac{5}{2}} - \frac{1}{4} (\alpha\beta^2 Y + \alpha\beta X) \left( -\frac{240\zeta\psi'(r)}{r^7} \right. \right. \\
& + \frac{12\xi\psi''(r)}{r^7} - \frac{8\zeta\psi'''(r)}{r^5} - \frac{8\zeta^2\psi''(r)}{r^7} - \frac{200\zeta\psi(r)\psi''(r)}{r^7} + \frac{576\zeta^2\psi^2(r)}{r^{10}} \\
& - \frac{256\xi^2\psi(r)\psi'(r)}{r^9} + \frac{1288\zeta\psi(r)\psi'(r)}{r^8} + \frac{36\zeta\psi'(r)\psi''(r)}{r^6} - \frac{200\zeta\psi'(r)}{r^7} \\
& + \frac{12\zeta\psi(r)\psi'''(r)}{r^6} + \frac{112\zeta^2\psi'(r)}{r^8} - \frac{448\zeta^2\psi(r)}{r^9} - \frac{1568\zeta\psi^2(r)}{r^9} \\
& - \frac{168\zeta\psi'(r)}{r^8} + \frac{672\zeta\psi(r)}{r^9} + \frac{80\zeta\psi''(r)}{r^6} + \frac{16\zeta^2\psi'^2(r)}{r^8} \\
& \left. \left. \left. + \frac{16\zeta^2\psi(r)\psi''(r)}{r^8} \right) \right) / Y^{\frac{3}{2}} \right), \tag{A3}
\end{aligned}$$

where

$$\begin{aligned}
X &= \left( \frac{12\zeta\psi(r)\psi'(r)}{r^6} - \frac{8\zeta^2\psi(r)}{r^7} - \frac{28\zeta\psi(r)^2}{r^7} + \frac{12\zeta\psi(r)}{r^7} - \frac{8\zeta\psi'(r)}{r^5} \right. \\
& \left. + \frac{8\zeta^2\psi(r)^2}{r^8} \right), \\
Y &= \left( \frac{3\zeta}{r^3} \left( 1 - \frac{\psi(r)}{r} \right) + \frac{2\zeta}{r^4} \left( 1 - \frac{\psi(r)}{r} \right) + \frac{2}{r^2} \left( 1 - \frac{\psi(r)}{r} \right) \right).
\end{aligned}$$

For isotropic fluid, we obtain the following equation

$$\begin{aligned}
& (-1 + (\alpha A)/(A^2 + \beta B)^{\frac{1}{2}}) \left( \frac{2}{r^2} \left( 1 - \frac{2\psi(r)}{r} \right) + \frac{4\zeta}{r^3} \left( 1 - \frac{\psi(r)}{r} \right) \right) + (6\zeta \\
& \times \left( 1 - \frac{\psi(r)}{r} \right)^2 \alpha\beta^2 C)/(r^4(A^2 + \beta B)^{\frac{3}{2}}) - \left( \frac{1}{r} \left( 2 - \frac{\psi(r)}{r} - \frac{\psi'(r)}{r} \right) \right) \\
& \times \left( \frac{\zeta}{r^2} + \frac{1}{r} \right) + 2 \left( 1 - \frac{\psi(r)}{r} \right) \left( \frac{\zeta^2}{r^4} - \frac{2\zeta}{r^3} \right) \left( -1 + (\alpha A)/(A^2 + \beta
\end{aligned}$$

$$\begin{aligned}
& \times B)^{\frac{1}{2}}) - 2 \left(1 - \frac{\psi(r)}{r}\right) \left(\frac{\zeta}{r^2} + \frac{1}{r}\right) (-\alpha A^2)/(A^2 + \beta B)^{\frac{3}{2}} + \alpha/(A^2 \\
& + \beta B)^{\frac{1}{2}}) \left(-\frac{9\zeta}{r^4} \left(1 - \frac{\psi(r)}{r}\right) + \frac{3\zeta}{r^3} \left(-\frac{\psi'(r)}{r} + \frac{\psi(r)}{r^2}\right) - \frac{8\zeta}{r^5} \left(1 - \frac{\psi(r)}{r}\right) \right. \\
& + \left. \frac{2\zeta}{r^4} \left(-\frac{\psi'(r)}{r} + \frac{\psi(r)}{r^2}\right) - \frac{4}{r^3} \left(1 - \frac{\psi(r)}{r}\right) + \frac{2}{r^2} \left(-\frac{\psi'(r)}{r} + \frac{\psi(r)}{r^2}\right) \right) \\
& + \frac{1}{4} \left( \left( \frac{12\zeta}{r^4} \left(\psi'(r) - \frac{\psi(r)}{r^2}\right) \left(1 - \frac{\psi(r)}{r}\right) - \frac{8}{r} \left(\frac{\zeta^2}{r^4} - \frac{2\zeta}{r^3}\right) \left(1 - \frac{\psi(r)}{r}\right) \right)^2 \right. \\
& \left. - \frac{\psi(r)}{r} \right)^2 \alpha \beta^2 C \Big) / (A^2 + \beta B)^{\frac{3}{2}} + \frac{1}{r^3} \left( 8\zeta \left(1 - \frac{\psi(r)}{r}\right) \right)^2 \left( \frac{3}{8} (\alpha \beta^3 C^2) \right. \\
& / (A^2 + \beta B)^{\frac{5}{2}} - \frac{1}{4} \left( \alpha \beta^2 \left( -\frac{240\zeta\psi'(r)}{r^7} - \frac{8\zeta^2\psi''(r)}{r^7} - \frac{8\zeta\psi'''(r)}{r^5} \right. \right. \\
& + \frac{12\zeta\psi''(r)}{r^7} - \frac{200\zeta\psi(r)\psi''(r)}{r^7} + \frac{1288\zeta\psi(r)\psi'(r)}{r^8} - \frac{256\zeta^2\psi(r)\psi'(r)}{r^9} \\
& + \frac{36\zeta\psi'(r)\psi''(r)}{r^6} - \frac{200\zeta\psi'^2(r)}{r^7} + \frac{12\zeta\psi(r)\psi'''(r)}{r^6} + \frac{112\zeta^2\psi'(r)}{r^8} \\
& - \frac{448\zeta^2\psi(r)}{r^9} - \frac{1568\zeta\psi^2(r)}{r^9} - \frac{168\zeta\psi'(r)}{r^8} + \frac{672\zeta\psi(r)}{r^9} + \frac{80\zeta\psi''(r)}{r^6} \\
& \left. \left. + \frac{16\zeta^2\psi'^2(r)}{r^8} + \frac{16\zeta^2\psi(r)\psi''(r)}{r^8} + \frac{576\zeta^2\psi^2(r)}{r^{10}} \right) \right) / (A^2 + \beta B)^{\frac{3}{2}}) = 0,
\end{aligned}$$

where

$$\begin{aligned}
A &= \frac{3\zeta}{r^3} \left(1 - \frac{\psi(r)}{r}\right) + \frac{2\zeta}{r^4} \left(1 - \frac{\psi(r)}{r}\right) + \frac{2}{r^2} \left(1 - \frac{\psi(r)}{r}\right). \\
B &= \frac{12A\psi(r)\psi'(r)}{r^6} - \frac{8A^2\psi(r)}{r^7} - \frac{28A\psi^2(r)}{r^7} + \frac{12A\psi(r)}{r^7} - \frac{8A\psi'(r)}{r^5} \\
&+ \frac{8A^2\psi^2(r)}{r^8}. \\
C &= \frac{12\zeta(\psi'(r))^2}{r^6} + \frac{12\zeta\psi(r)\psi''(r)}{r^6} - \frac{128\zeta\psi(r)\psi'(r)}{r^7} - \frac{8\zeta^2\psi'(r)}{r^7} + \frac{56\zeta^2\psi(r)}{r^8} \\
&+ \frac{196\zeta\psi^2(r)}{r^8} + \frac{12\zeta\psi'(r)}{r^7} - \frac{84\zeta\psi(r)}{r^8} - \frac{8\zeta\psi''(r)}{r^5} + \frac{40\zeta\psi'(r)}{r^6} - \frac{64\zeta^2\psi^2(r)}{r^9} \\
&+ \frac{16\zeta^2\psi(r)\psi'(r)\psi}{r^8}.
\end{aligned}$$

For barotropic fluid, we obtain the following equation as

$$\begin{aligned}
& A - \alpha(A^2 + \beta B)^{\frac{1}{2}} + \left( \frac{2}{r^2} \left( 1 - \frac{2\psi(r)}{r} \right) + \frac{4\zeta}{r^3} \left( 1 - \frac{\psi(r)}{r} \right) \right) (\alpha A \\
& / (A^2 + \beta B)^{\frac{1}{2}}) + \frac{1}{2}(B\alpha\beta)/(A^2 + \beta B)^{\frac{1}{2}} + (6\zeta \left( 1 - \frac{\psi(r)}{r} \right)^2 \alpha\beta^2 C) \\
& / (r^4(A^2 + \beta B)^{\frac{3}{2}}) - \mu(-A + \alpha(A^2 + B)^{\frac{1}{2}} - A(-1 + (\alpha A)/(A^2 + \beta \\
& \times B)^{\frac{1}{2}}) - \frac{1}{2}(B\alpha\beta)/(A^2 + \beta B)^{\frac{1}{2}} + \frac{1}{r^2}(2\psi'(r)(-1 + (\alpha A)/(A^2 + \beta \\
& \times B)^{\frac{1}{2}})) - \frac{1}{r}(4 \left( 1 - \frac{\psi(r)}{r} \right) (-\alpha A^2)/(A^2 + \beta B)^{\frac{3}{2}} + \alpha/(A^2 + \beta \\
& \times B)^{\frac{1}{2}}) \left( -\frac{9\zeta}{r^4} \left( 1 - \frac{\psi(r)}{r} \right) + \frac{3\zeta}{r^3} \left( -\frac{\psi'(r)}{r} + \frac{\psi(r)}{r^2} \right) - \frac{8\zeta}{r^5} \left( 1 - \frac{\psi(r)}{r} \right) \right) \\
& + \frac{2\zeta}{r^4} \left( -\frac{\psi'(r)}{r} + \frac{\psi(r)}{r^2} \right) - \frac{4}{r^3} \left( 1 - \frac{\psi(r)}{r} \right) + \frac{2}{r^2} \left( -\frac{\psi'(r)}{r} + \frac{\psi(r)}{r^2} \right) \Big) \\
& - \left( \left( \frac{5\psi(r)}{r} - 2 - \frac{3\psi^2(r)}{r^2} - 3\psi'(r) \left( 1 - \frac{\psi(r)}{r} \right) \right) \alpha\beta^2 C \right) / (r^3(A^2 \\
& + \beta B)^{\frac{3}{2}}) + \frac{1}{r^2}(8(1 - \frac{\psi(r)}{r})(2 - \frac{\psi'(r)}{r}))(\frac{3}{8}(\alpha\beta^3 C^2)/(A^2 + 2B)^{\frac{5}{2}} - \frac{1}{4} \\
& \times (\alpha\beta^2(-\frac{240\zeta\psi'(r)}{r^7} - \frac{168\zeta\psi'(r)}{r^8} - \frac{8\zeta^2\psi''(r)}{r^7} - \frac{8\zeta\psi'''(r)}{r^5} - \frac{12\zeta\psi''(r)}{r^7} \\
& - \frac{200\zeta\psi(r)\psi''(r)}{r^7} + \frac{1288\zeta\psi(r)\psi'(r)}{r^8} - \frac{256\zeta^2\psi(r)\psi'(r)}{r^9} + \frac{36\zeta\psi'(r)\psi''(r)}{r^6} \\
& - \frac{200\zeta\psi^2(r)}{r^7} + \frac{12\zeta\psi(r)\psi'''(r)}{r^6} + \frac{112\zeta^2\psi'(r)}{r^8} - \frac{448\zeta^2\psi(r)}{r^9} - \frac{1568\zeta\psi^2(r)}{r^9} \\
& + \frac{672\zeta\psi(r)}{r^9} + \frac{80\zeta\psi''(r)}{r^6} + \frac{16\zeta^2\psi'^2(r)}{r^8} + \frac{16\zeta^2\psi(r)\psi''(r)}{r^8} + \frac{576\zeta^2\psi^2(r)}{r^{10}})) \\
& / (A^2 + \beta B)^{\frac{3}{2}}) = 0.
\end{aligned}$$

For traceless fluid, we obtain the following equation as

$$\begin{aligned}
& (6\zeta \left( 1 - \frac{\psi(r)}{r} \right)^2 \alpha\beta^2 C) / (r^4(A^2 + \alpha_2 B)^{\frac{3}{2}}) + \frac{8}{r^2} \left( 1 - \frac{\psi(r)}{r} \right) - \frac{1}{2} \\
& \times (B\alpha\beta^2 C) / (A^2 + \beta B)^{\frac{3}{2}} - \frac{1}{r^3}(16\zeta \left( 1 - \frac{\psi(r)}{r} \right)^2 (\frac{3}{8}(\alpha\beta^3 A^2) / (A^2 \\
& + \beta B)^{\frac{5}{2}} - \frac{1}{4} \left( \alpha\beta^2 \left( -\frac{240\zeta\psi'(r)}{r^7} - \frac{8\zeta^2\psi''(r)}{r^7} - \frac{8\zeta\psi'''(r)}{r^5} + \frac{12\zeta\psi''(r)}{r^7} \right) \right)
\end{aligned}$$

$$\begin{aligned}
& - \frac{200\zeta\psi(r)\psi''(r)}{r^7} + \frac{1288\zeta\psi(r)\psi'(r)}{r^8} - \frac{256\zeta^2\psi(r)\psi'(r)}{r^9} - \frac{200\zeta\psi'^2(r)}{r^7} \\
& + \frac{36\zeta\psi'(r)\psi''(r)}{r^6} + \frac{12\zeta\psi(r)\psi'''(r)}{r^6} + \frac{112\zeta^2\psi'(r)}{r^8} - \frac{448\zeta^2\psi(r)}{r^9} \\
& - \frac{1568\zeta\psi^2(r)}{r^9} - \frac{168\zeta\psi'(r)}{r^8} + \frac{672\zeta\psi(r)}{r^9} + \frac{80\zeta\psi''(r)}{r^6} + \frac{16\zeta^2\psi'^2(r)}{r^8} \\
& + \left. \frac{16\zeta^2\psi(r)\psi''(r)}{r^8} + \frac{576\zeta^2\psi^2(r)}{r^{10}} \right) / (A^2 + \beta B)^{\frac{3}{2}}) - \frac{1}{r^2} \left( 8 \left( 1 - \frac{\psi(r)}{r} \right) \right. \\
& \times \left. \left( 2 - \frac{\psi(r)}{r} \right) \right) \left( \frac{3}{8} (\alpha\beta^3 C^2) / (A^2 + \beta B)^{\frac{5}{2}} - \frac{1}{4} (\alpha\beta^2 \left( -\frac{240\zeta\psi'(r)}{r^7} \right. \right. \right. \\
& - \frac{8\zeta^2\psi''(r)}{r^7} - \frac{8\zeta\psi'''(r)}{r^5} + \frac{12\zeta\psi''(r)}{r^7} - \frac{200\zeta\psi(r)\psi''(r)}{r^7} - \frac{256\zeta^2\psi(r)\psi'(r)}{r^9} \\
& + \frac{1288\zeta\psi(r)\psi'(r)}{r^8} + \frac{36\zeta\psi'(r)\psi''(r)}{r^6} - \frac{200\zeta\psi'^2(r)}{r^7} + \frac{12\zeta\psi(r)\psi'''(r)}{r^6} \\
& + \frac{112\zeta^2\psi'(r)}{r^8} - \frac{448\zeta^2\psi(r)}{r^9} - \frac{1568\zeta\psi^2(r)}{r^9} - \frac{168\zeta\psi'(r)}{r^8} + \frac{672\zeta\psi(r)}{r^9} \\
& + \left. \frac{80\zeta\psi''(r)}{r^6} + \frac{16\zeta^2\psi'^2(r)}{r^8} + \frac{16\zeta^2\psi(r)\psi''(r)}{r^8} - \frac{576\zeta^2\psi^2(r)}{r^{10}} \right) \Big) / (A^2 + \alpha \\
& \times B)^{\frac{3}{2}}) - \frac{1}{r^2} (2\psi'(r)(-1 + (\alpha(\frac{3\zeta}{r^3}(1 - \frac{\psi(r)}{r}) + \frac{2\zeta}{r^4}(1 - \frac{\psi(r)}{r}) + \frac{2}{r^2}(1 \\
& - \frac{\psi(r)}{r})))) / (A^2 + \beta B)^{\frac{1}{2}}) + ((\frac{5\psi(r)}{r} - 2 - \frac{3\psi^2(r)}{r^2} - 3\psi'(r)(1 - \frac{\psi(r)}{r})) \\
& \times \alpha\beta^2 C) / (r^3(A^2 + \beta B)^{\frac{3}{2}}) + 2(\frac{1}{r}(2 - \frac{\psi(r)}{r} - \frac{\psi'(r)}{r})(\frac{\zeta}{r^2} + \frac{1}{r}) + 2(1 \\
& - \frac{\psi(r)}{r})(\frac{\zeta^2}{r^4} - \frac{2\zeta}{r^3}))(-1 + (\alpha A) / (A^2 + \beta B)^{\frac{1}{2}}) - 4\alpha(A^2 + \beta B)^{\frac{1}{2}} \\
& + A(-1 + (\alpha A) / (A^2 + \beta B)^{\frac{1}{2}}) + (\frac{2}{r^2}(1 - \frac{2\psi(r)}{r}) + \frac{4\zeta}{r^3}(1 - \frac{\psi(r)}{r}))(-1 \\
& + (\alpha A) / (A^2 + \beta B)^{\frac{1}{2}}) + \frac{1}{r}(4(1 - \frac{\psi(r)}{r})(-\alpha A^2) / (A^2 + \alpha\beta B)^{\frac{3}{2}} + \alpha \\
& / (A^2 + \beta B)^{\frac{1}{2}})(-\frac{9\zeta}{r^4}(1 - \frac{\psi(r)}{r}) + \frac{3\zeta}{r^3}(\frac{\psi'(r)}{r} + \frac{\psi(r)}{r^2}) - \frac{8\zeta}{r^5}(1 \\
& - \frac{\psi(r)}{r}) + \frac{2\zeta}{r^4}(\frac{\psi'(r)}{r} + \frac{\psi(r)}{r^2}) - \frac{4}{r^3}(1 - \frac{\psi(r)}{r}) + \frac{2}{r^2}(\frac{\psi'(r)}{r} \\
& + \frac{\psi(r)}{r^2})) + (2B\alpha\beta) / (A^2 + \beta B)^{\frac{1}{2}} + 4(1 - \frac{\psi(r)}{r}) \left( \frac{\zeta}{r^2} + \frac{1}{r} \right) (-\alpha
\end{aligned}$$

$$\begin{aligned}
& \times A^2)/(A^2 + \beta B)^{\frac{3}{2}} + \alpha/(A^2 + \beta B)^{\frac{1}{2}}) \left( -\frac{9\zeta}{r^4} \left( 1 - \frac{\psi(r)}{r} \right) + \frac{3\zeta}{r^3} \left( \frac{\psi(r)}{r^2} \right. \right. \\
& - \left. \left. \frac{\psi'(r)}{r} \right) - \frac{8\zeta}{r^5} \left( 1 - \frac{\psi(r)}{r} \right) + \frac{2\zeta}{r^4} \left( -\frac{\psi'(r)}{r} + \frac{\psi(r)}{r^2} \right) - \frac{4}{r^3} \left( 1 - \frac{\psi(r)}{r} \right) \right) \\
& + \frac{2}{r^2} \left( -\frac{\psi'(r)}{r} + \frac{\psi(r)}{r^2} \right) + \frac{12\zeta}{r^3} \left( 1 - \frac{\psi(r)}{r} \right) + \frac{8\zeta}{r^4} \left( 1 - \frac{\psi(r)}{r} \right) = 0.
\end{aligned}$$

## References

- [1] Maeda, H.: *Class. Quantum Grav.* **23**(2006)2155.
- [2] Nojiri, S. and Odintsov, S.D.: *Int. J. Geom. Methods Mod. Phys.* **04**(2007)115.
- [3] Ferraro, R. and Fiorini, F.: *Phys. Rev. D* **75**(2007)084031; **78**(2008)124019.
- [4] Harko, T., Lobo, F.S.N., Nojiri, S. and Odintsov, S.D.: *Phys. Rev. D* **84**(2011)024020.
- [5] Kofinas, G. and Saridakis, E.N.: *Phys. Rev. D* **90**(2014)084044.
- [6] Kofinas, G., Leon, G. and Saridakis, E.N.: *Class. Quantum Grav.* **31**(2014)175011.
- [7] Chattopadhyay, S., Jawad, A., Momeni, D. and Myrzakulov, R.: *Astrophys. Space Sci.* **353**(2014)279; Jawad, A. and Debnath, U.: *Commun. Theor. Phys.* **64**(2015)145; Sharif, M. and Nazir, K.: *Mod. Phys. Lett. A* **31**(2016)1650148; Capozziello, S., Laurentis, M.D. and Dialektopoulos, K.F.: *Eur. Phys. J. C* **76**(2016)629.
- [8] Wang, A. and Letelier, P.S.: *Prog. Theor. Phys.* **94**(1995)137.
- [9] Kim, S.W. and Kim, S.P.: *Phys. Rev. D* **58**(1998)087703.
- [10] Bronnikov, K.A. and Kim, S.W.: *Phys. Rev. D* **67**(2003)064027.
- [11] Lobo, F.S.N.: *Phys. Rev. D* **73**(2006)064028.
- [12] Rahaman, F., Islam, S., Kuhfitting, P.K.F. and Ray, S.: *Phys. Rev. D* **86**(2012)106010.

- [13] Abreu, E.M.C. and Sasaki, N.: arXiv:1207.7130.
- [14] Lobo, F.S.N. and Oliveira, M.A.: Phys. Rev. D **80**(2009)104012.
- [15] Böhmer, C.G., Harko, T. and Lobo, F.S.N.: Phys. Rev. D **85**(2012)044033.
- [16] Sharif, M. and Rani, S.: Phys. Rev. D **88**(2013)123501.
- [17] Sharif, M. and Nazir, K.: Mod. Phys. Lett. A **32**(2017)1750083.
- [18] Sharif, M. and Rani, S.: Gen. Relativ. Gravit. **45**(2013)2389.
- [19] Sharif, M. and Zahra, Z.: Astrophys. Space. Sci. **348**(2013)275.
- [20] Sharif, M. and Ikram, A.: Int. J. Mod. Phys. D **24**(2015)1550003.
- [21] Zubair, M., Waheed, S. and Ahmad, Y.: Eur. Phys. J. C **76**(2016)444.
- [22] Morris, M. and Thorne, A.: Am. J. Phys. **56**(1988)395.
- [23] Carroll, S.: *Spacetime and Geometry: An Introduction to General Relativity* (Addison-Wesley, 2004).
- [24] Jamil, M., Momeni, D. and Myrzakulov, R.: Eur. Phys. J. C **73**(2013)2267.
- [25] Pavlovic, P. and Sossich, M.: Eur. Phys. J. C **75**(2015)117.
- [26] Kainulainen, K. et al.: Phys. Rev. D **76**(2007)024020.